SECTION II. TASK 2. SUBMODEL DEVELOPMENT AND EVALUATION

Objectives

The objectives of this task are to develop or adapt advanced physics and chemistry submodels for the reactions of coal in an entrained-bed and a fixed-bed reactor and to validate the submodels by comparison with laboratory scale experiments.

Task Outline

The development of advanced submodels for the entrained-bed and fixed-bed reactor models will be organized into the following categories: a) Coal Chemistry (including coal pyrolysis chemistry, char formation, particle mass transfer, particle thermal properties, and particle physical behavior); b) Char Reaction Chemistry at high pressure; c) Secondary Reactions of Pyrolysis Products (including gas-phase cracking, soot formation, ignition, char burnout, sulfur capture, and tar/gas reactions); d) Ash Physics and Chemistry (including mineral characterization, evolution of volatile, molten and dry particle components, and ash fusion behavior); e) Large Coal Particle Effects (including temperature, composition, and pressure gradients and secondary reactions within the particle, and the physical affects of melting, agglomeration, bubble formation and bubble transport; f) Large Char Particle Effects (including oxidation); g) SO_x-NO_x Submodel Development (including the evolution and oxidation of sulfur and nitrogen species); and h) SO_x and NO_x Model Evaluation.

II.A. SUBTASK 2.a. - COAL TO CHAR CHEMISTRY SUBMODEL DEVELOPMENT AND EVALUATION

Senior Investigator - David G. Hamblen
Advanced Fuel Research, Inc.
87 Church Street, East Hartford, CT 06108
(203) 528-9806

Objective

The objective of this subtask is to develop and evaluate, by comparison with laboratory experiments, an integrated and compatible submodel to describe the organic chemistry and physical changes occurring during the transformation from coal to char in coal conversion processes. Many of the data and some computer codes for this submodel are available, so it is expected that a complete integrated code will be developed during Phase I. Improvements in accuracy and efficiency will be pursued during Phase II.

Accomplishments

In order to further understand the role played by ion-exchangeable cations on char reactivity, samples of demineralized Zap coal were subjected to ion-exchange with Mg and Ca. This work is being done jointly under Subtasks 2.a, 2.c, and 2.d, which cover initial reactivity, char burnout and mineral catalytic effects, respectively. For the time being, it will be reported under Subtask 2.a. Chars were prepared by heating in a TGA at 30°C/min to 900°C or 1000°C and reactivity measurements were done in both air and CO_2. In both gases the loading of sufficient amounts of Mg or Ca produced a char which was equal or more reactive than chars produced from the raw coal.

Char samples obtained from drop tube experiments done with Pittsburgh Seam coal were prepared for SEM analysis by potting and polishing. The SEM photographs were taken and were analyzed to obtain quantitative information such as bubble size and wall thickness, which can be used for validation of the viscosity and swelling models. Our preliminary analysis indicates that maceral effects may be important.

Work resumed on the viscosity model and continued on using the FG-DVC model to model the baseline pyrolysis data obtained for the 10 coals from the EFR and TG-FTIR reactors, as well as from FIMS analysis at SRI International. Some refinements were made to the treatment of internal and external transport in the

model. Work was also done on comparing the FG-DVC model to the statistical model of Pugmire and Grant at the University of Utah which is based on percolation theory.

Entrained flow reactor experiments continued with three coals and additional FIMS analysis experiments were done at SRI.

Coal Characterization

Additional characterization of coal samples was done by doing ion-exchange and char reactivity experiments with various cations, swelling experiments with the Pittsburgh Seam bituminous coal and pyrolysis experiments in the TG-FTIR, EFR and FIMS reactors.

Char Reactivity

In order to further understand the roles played by the ion-exchangeable cations in char reactivity, a 200 x 325 mesh sieved fraction of Zap Indian Head, demineralized according to the standard Bishop and Ward (1958) technique, was subjected to ion-exchange with Mg and Ca, using a modification of the procedure by Hengel and Walker (1984). In the case of Mg, a 1.5M acetate salt solution was employed. In the case of Ca, the amount ion-exchanged onto the demineralized Zap lignite was controlled by using 0.5M, 1.0M and 1.5M acetate salt solutions. Slurries of 5 grams of demineralized Zap and 125 ml of the desired loading solution was stirred at 57°C for 5 1/2 hours. The solution was allowed to cool to room temperature and stirring was continued for an additional 22 1/2 hours. The slurry was filtered, washed with deionized water and dried at 105°C in a vacuum oven for approximately two hours.

The amount of cation exchanged was determined by x-ray analysis. Listed in Table II.A-1 are the mineral components for the raw, demineralized and cation loaded Zap Indian Head samples.

Char reactivity measurements (T_{cr}) were done both in air and in CO_2 and can be viewed in Table II.A-2. In the case of air reactivity, chars were prepared by heating in N_2 at 30°C/min to 900°C. In the case of CO_2 reactivity, chars were prepared by heating in N_2 at 30°C/min until 1000°C was achieved.

In both air and CO_2, the demineralized Zap char is far less reactive (higher T_{cr}) than the raw Zap char. As discussed in previous reports, this is probably due

Table II.A-1. Mineral Components in Raw, Demineralized and Cation Loaded Zap Indian Head Lignite Samples.

	Raw Zap	Demin. Zap	Mg Loaded Demin. Zap	0.5M Ca Loaded Demin. Zap	1.0M Ca Loaded Demin. Zap	1.5M Ca Loaded Demin. Zap
Na	0.13	-0.03	-0.17	-0.02	-0.03	-0.03
Mg	0.46	0.05	2.33	0.05	0.03	0.03
Al	0.46	0.04	-0.06	0.03	0.03	0.04
Si	0.84	0.09	0.15	0.05	0.06	0.09
K	0.04	0.01	0.00	-0.02	-0.02	-0.02
Ca	1.26	0.10	0.02	3.31	3.70	4.08
Ti	0.04	0.01	0.00	0.03	0.01	0.00
S(o)	0.47	0.49	0.42	0.38	0.41	0.44
S(m)	0.31	0.09	0.12	0.14	0.18	0.08
Fe*	0.45	0.05	0.06	0.02	0.05	0.06
Ash	8.62	0.80	3.91	6.32	7.10	7.41

* Non-Pyritic Iron

Table IIA - 2. Reactivity Measurements for Raw, Demineralized and Cation Loaded Demineralized Zap Indian Head Lignite Samples.

	900°C N_2 Char T_{cr} °C in Air	1000°C N_2 Char T_{cr} °C in CO_2
Raw Zap	420, 418	849
Demineralized Zap	528	992
Mg Loaded Demin. Zap	433, 424	909, 908
0.5M Ca Loaded Demin Zap	413	---
1.0M Ca Loaded Demin Zap	426	---
1.5M Ca Loaded Demin. Zap	433, 434	819, 821

to the removal of the organically bound alkali metals which are thought to dominate char reactivity in coals possessing more than 8% O_2. If this is true, then cation loading should result in the restoration of char reactivity.

The 1.5M Ca and Mg loadings effectively increased the demineralized Zap char air reactivity. In both cases, the loaded samples proved to be almost as reactive as the raw coal. A plot of T_{cr} (°C) in air versus Ca weight percent obtained from the raw, demineralized and the 0.5M 1.0M and 1.5M loaded Zap samples (Fig. II.A-1) suggests that calcium's ability to promote char reactivity in air decreases at higher loadings. Furthermore, the optimum level of Ca for increased char reactivity exists between 1.26 wt% and 3.31 wt%. This differs from the results of Hippo et al. (1979) who found that the steam reactivity increased linearly with Ca loading up to 13 wt% Ca in the char, even when allowing for a factor of two difference between loadings on a char basis and a coal basis. This may be due to the difference in mechanisms between the steam and O_2 gasification reactions. We will be examining additional Ca loading levels to better establish the saturation levels.

When gasification took place in CO_2, the Ca and Mg loadings again effectively increased the demineralized Zap char reactivity. In the case of Mg, the loaded demineralized Zap sample was 60°C less reactive than the raw Zap lignite while in the case of Ca, the loaded demineralized sample actually became 30°C more reactive than the raw Zap sample.

Swelling Experiments

In this quarter, samples of the 200 x 325 mesh sieved fraction of Pittsburgh No. 8 bituminous coal were subjected to low temperature pyrolysis in the drop tube furnace described in the last quarterly report. Drop tube temperatures ranged from 450°C to 700°C.

The TGA was employed to determine the amount of volatiles remaining in each of the chars collected. Char samples were heated in N_2 at 30°C/min to 900°C. The percent volatiles released (DAF) in the TGA is plotted in Fig. II.A-2a as a function of drop tube temperature. Results from the set of drop tube chars presented in the Fifth Quarterly Report are included here for comparison. If a plot is made using the volatiles released by heating to 550°C, as shown in Fig. II.A.2b, the rapid tar loss that occurs in this temperature range is more evident.

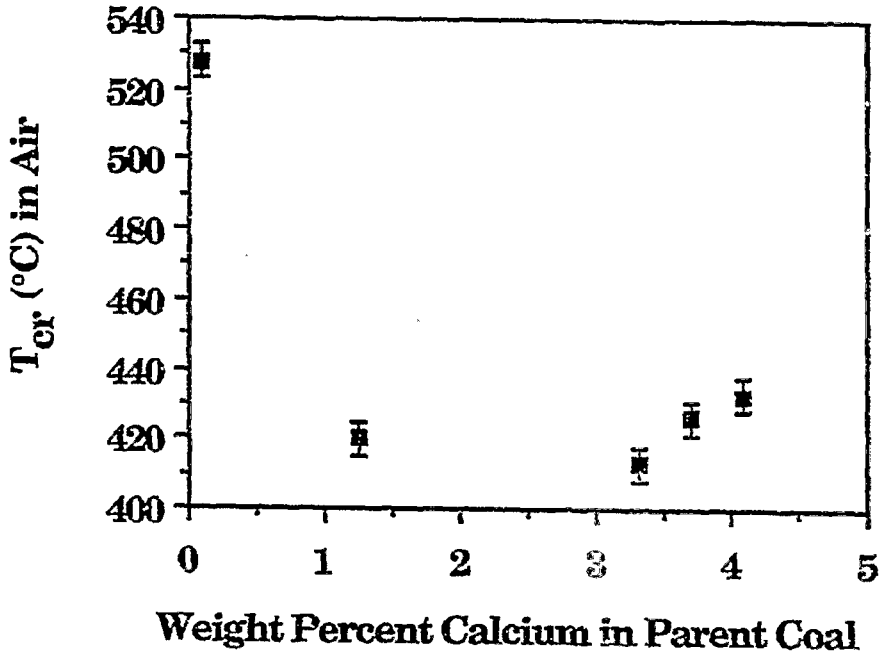

Figure II.A-1. Variation of Reactivity in Air with Weight Percent Calcium in the Parent Coal.

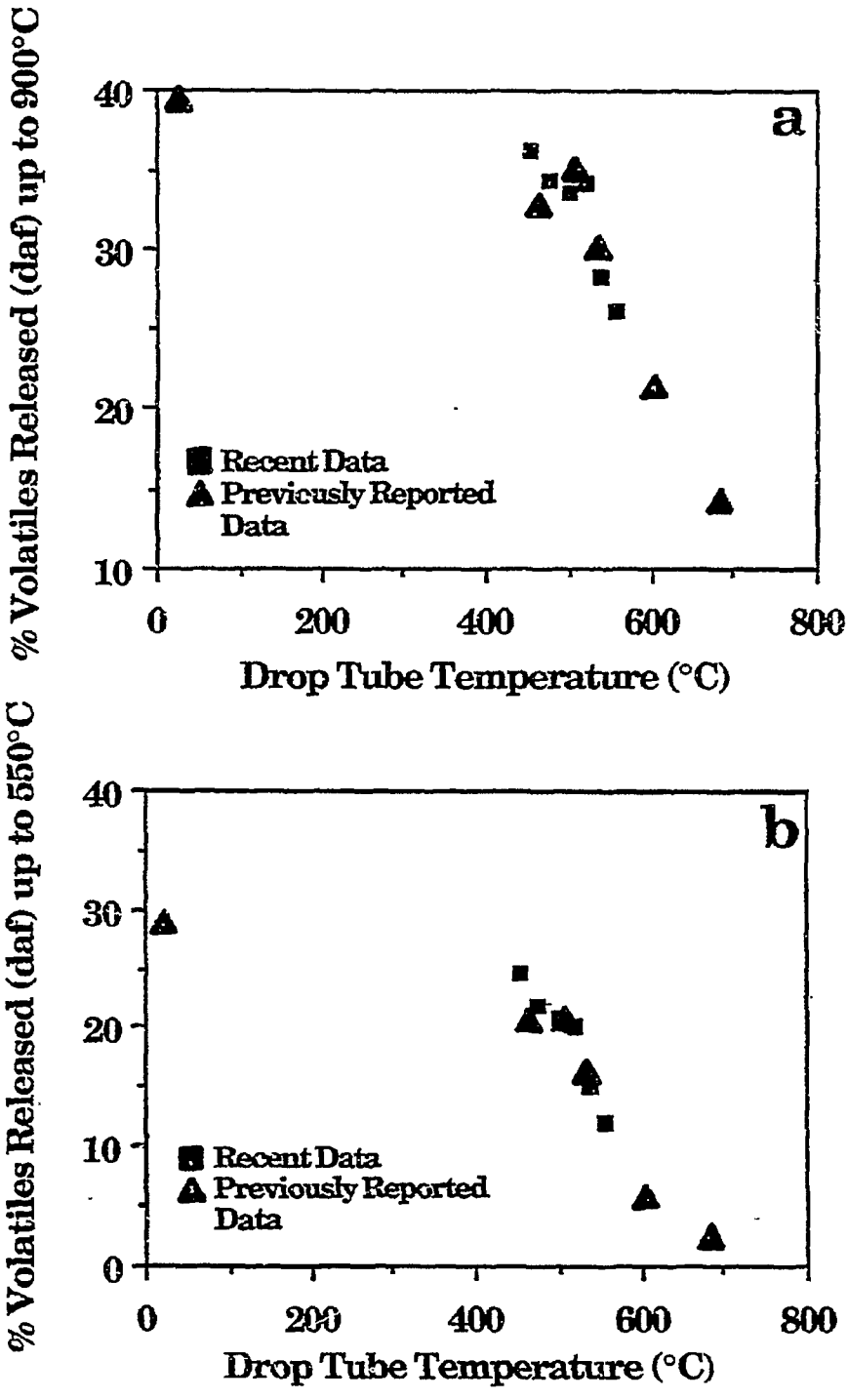

Figure II.A-2. Variation of Percent Volatiles Released (daf) for TGA Pyrolysis of the Chars Recovered from Drop Tube Experiments with Pittsburgh Seam Bituminous Coal. a) 30°C/min up to 900°C; b) 30°C/min up to 550°C.

The SEM was employed to obtain both external (Figs. II.A-3 to II.A-8) and internal (Figs. II.A-9) micrographs of the low temperature char particles. In order to micrograph the internal structure, the char particles were first subjected to potting and "cutting". This technique involved mixing approximately 20 mg of char sample and 1-2 ml of LR White hard grade acrylic resin in micron embedding mounts. With continued stirring, less than one drop of LR White accelerator was added to quicken polymerization. The potted samples were cured at 58°C for a twenty-four hour period and "cut" with a single edged razor blade.

Examination of the external micrographs suggests that three different pyrolysis pathways exist. Particles seem to undergo either 1) rapid swelling and cenosphere formation at lower temperatures or 2) gradual surface flowing, swelling and cenosphere formation or, 3) no obvious swelling and lack cenosphere formation even at higher temperatures.

A possible explanation for the differences in char morphology could be due to the differences in maceral content. According to data obtained from Karl Vorres at Argonne National Laboratories, Pittsburgh No. 8 bituminous coal contains 7% liptinite, 85% vitrinite and 8% inertinite (Vorres, 1988). In lower rank coals where the properties of macerals differ, Richard Neavel describes the inertinite as being carbon rich when compared to the vitrinite of the same coal, and the liptinite as being comparatively hydrogen rich (Neavel, 1981).

If one assumes that for finely ground particles, most of the particles contain single maceral types, one might expect 7% of the particles to be composed of liptinite and undergo rapid swelling, 85% of the particles to be composed of vitrinite and undergo a more gradual swelling, and 8% of the particles to be composed of inertinite and lack swelling qualities.

Assuming the SEM micrographs displayed in Figs. II.A-3 to II.A-8 are representative of the char particles collected at each drop tube temperature, approximations can be made regarding maceral content. In the 454°C char case, 4 $\pm$ 1 out of 37 particles have under gone cenosphere formation. In other words, 8-12% of the particles are perhaps liptinite in composition. Similarly, at 478°C, 6 $\pm$ 2 out of 50 particles have formed cenospheres or 8-16% of the particles are possibly liptinite in composition. In the 502 and 519°C char cases, the majority of the particles (possibly all the liptinite and vitrinite particles) have either demonstrated some form of swelling or have already formed cenospheres. At 558°C, 6 $\pm$ 2 out of 49 particles or 8 - 16% of the particles have not demonstrated any

Figure II.A-3. SEM Micrograph of a 454°C Drop Tube Char of Pittsburgh No.8 Bituminous Coal. Magnification: 300X.

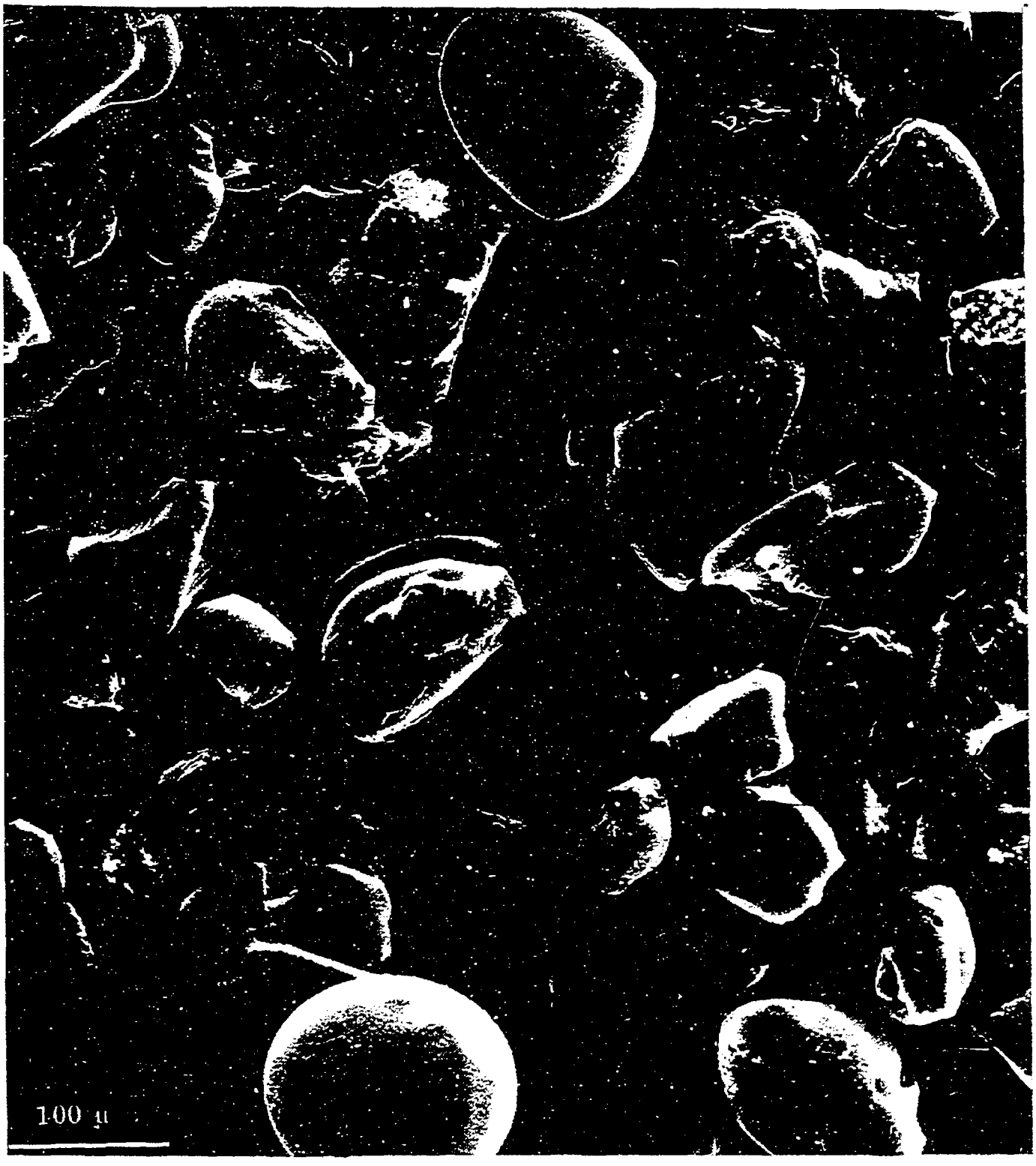

Figure II.A-4. SEM Micrograph of a 478°C Drop Tube Char of Pittsburgh No.8 Bituminous Coal. Magnification: 300X.

Figure II.A-5. SEM Micrograph of a 502°C Drop Tube Char of Pittsburgh No.8 Bituminous Coal. Magnification: 300X.

Figure II.A-6. SEM Micrograph of a 519°C Drop Tube Char of Pittsburgh No.8 Bituminous Coal. Magnification: 300X.

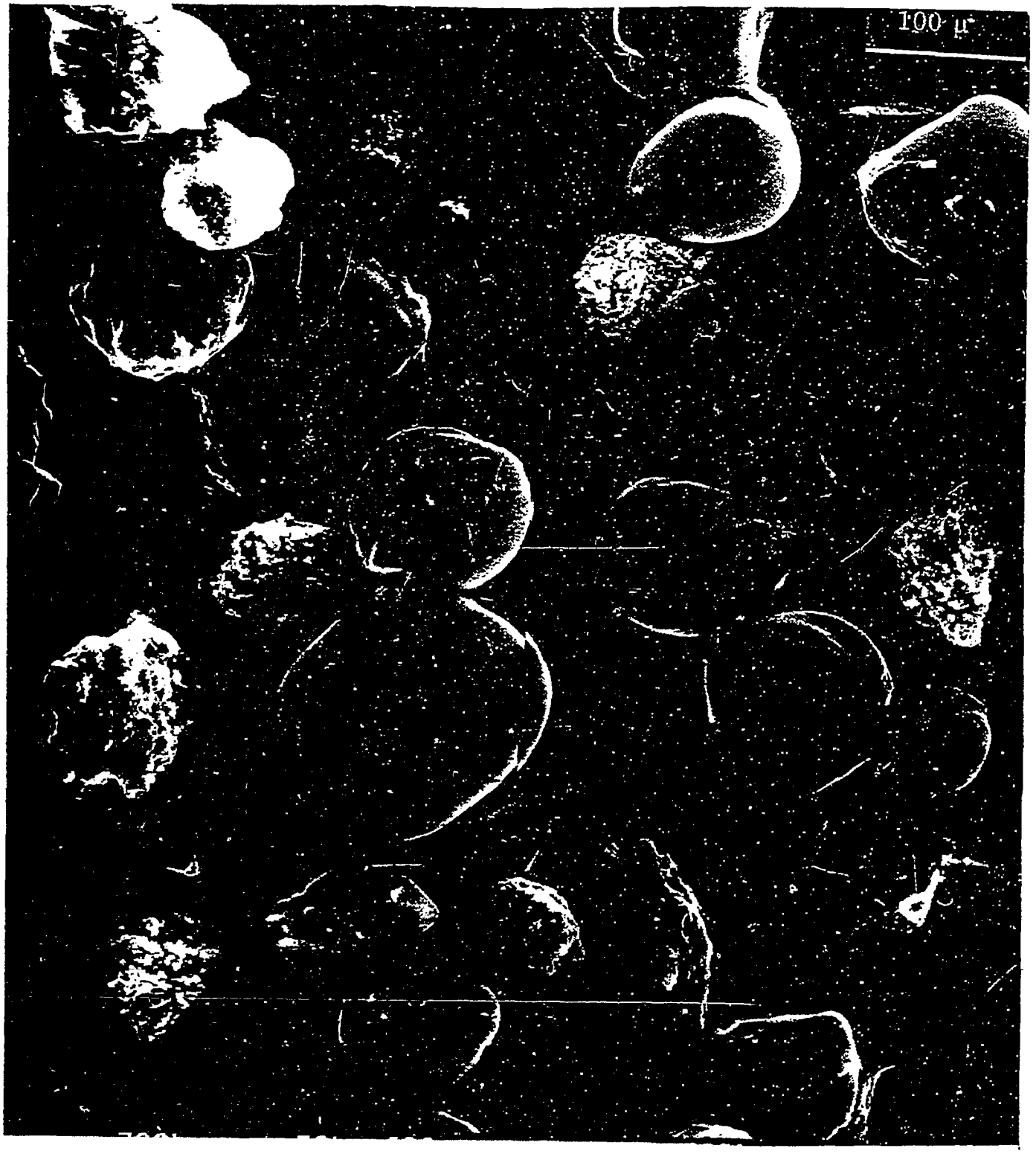

Figure II.A-7. SEM Micrograph of a 538°C Drop Tube Char of Pittsburgh No.8 Bituminous Coal. Magnification: 300X.

Figure II.A-8. SEM Micrograph of a 558°C Drop Tube Char of Pittsburgh No.8 Bituminous Coal. Magnification: 300X.

indications of surface melting or swelling and are probably inertinite in composition.

Figure II.A-9 displays the internal structures which the majority of the particles possess at various stages of pyrolysis. In Fig. II.A-9a, the particle is quite angular and has micropores of approximately one micron in diameter. In Figs. II.A-9b and II.A-9c, the particles have begun to lose their angularity and the micropores have begun to increase in size, forming bubbles ranging from approximately 5-15 microns in diameter. In Figs. II.A-9d and II.A-9e, the bubbles have both decreased in quantity and increased in diameter to as large as 85 microns. Finally, in Fig. II.A-f, a hollow cenosphere of approximately 110 micron diameter has formed.

TG-FTIR Experiments

As reported previously, the TG-FTIR apparatus has been used to characterize the coal samples used in this program. Approximately 35 mg of coal sample was heated at 30°C/min, first to 150°C for drying and then to 900°C for pyrolysis. In the fifth quarterly report, results were reported for the tar evolution rates for the eight Argonne coal samples. These experiments were repeated with an improved temperature calibration for the instrument and better sealing against air leaks. The results are shown for the tar in Fig. II.A-10 and for CH_4, CO_2, CO, SO_2, and H_2O in Figs. II.A-10 to II.A-14, respectively. The coals are arranged on each plot according to the rank order given in Table II.A-3. The actual temperature-time profiles are given on the first plot in each figure.

The results show how the structure of the product gas evolution curves varies from simple in the case of hydrocarbons to complex in the case of oxygenated species. One reason is that the latter are likely to be influenced by mineral decomposition peaks. Of course this can be assessed to a large extent by running demineralized samples, which we are in the process of doing.

In order to determine how well pyrolysis of the Argonne coals agreed with the assumption of rank-insensitive kinetics, a compilation was made of the temperatures for maximum evolution rate for the evolution of the most consistently prominent peaks for each gaseous product. This was difficult in some cases because of the fact that numerous "subpeaks", shoulders and minor peaks were often present. However, it was the usual case that an identifiable peak appeared in the same

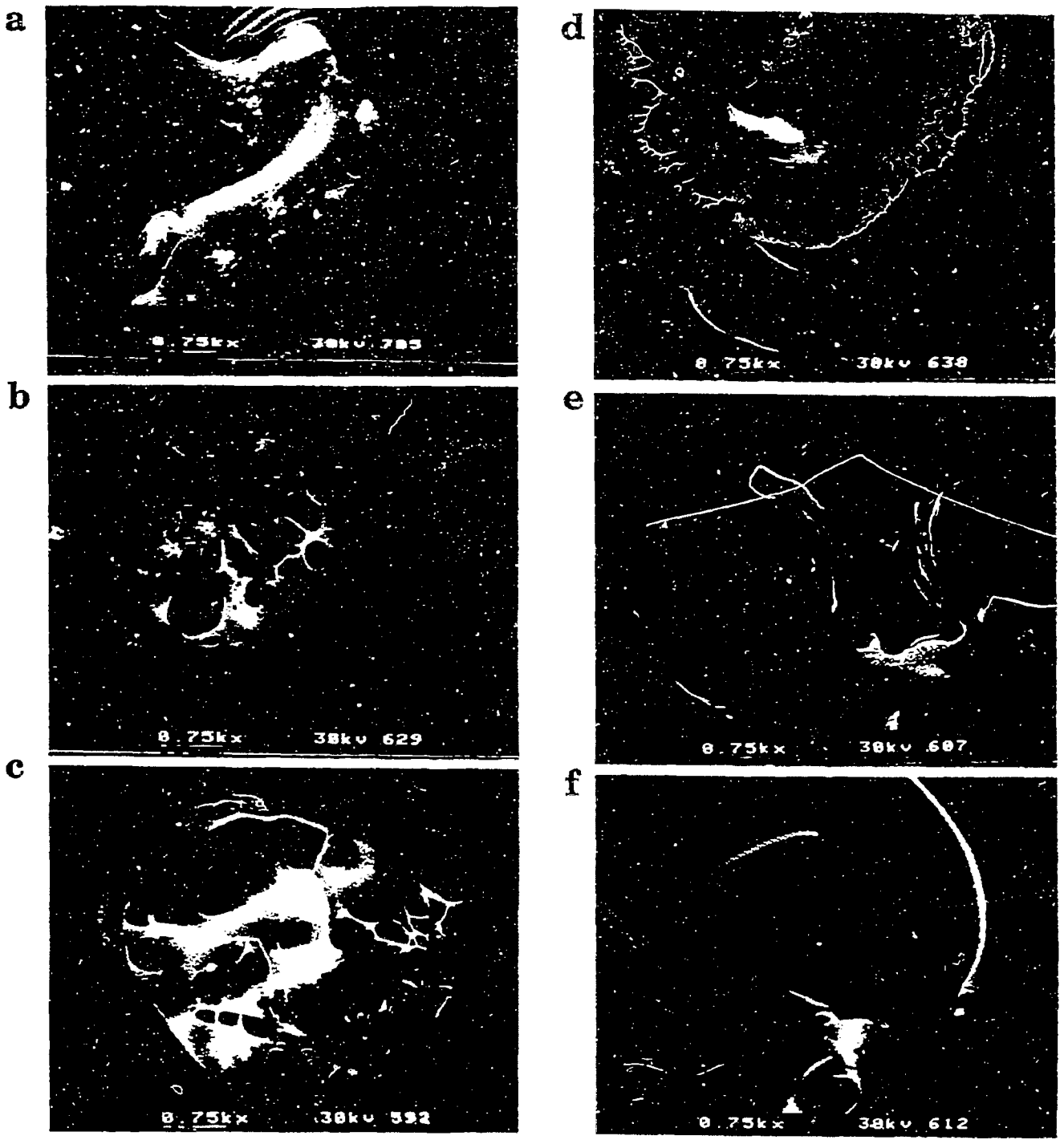

Figure II.A-9. Sem Micrographs of a) 454°C, b) 478°C, c) 454°C, d) 502°C, e) 538°C and f) 538°C, Drop Tube Chars of Pittsburgh No. 8 Bituminous Coal. Magnification: 75X.

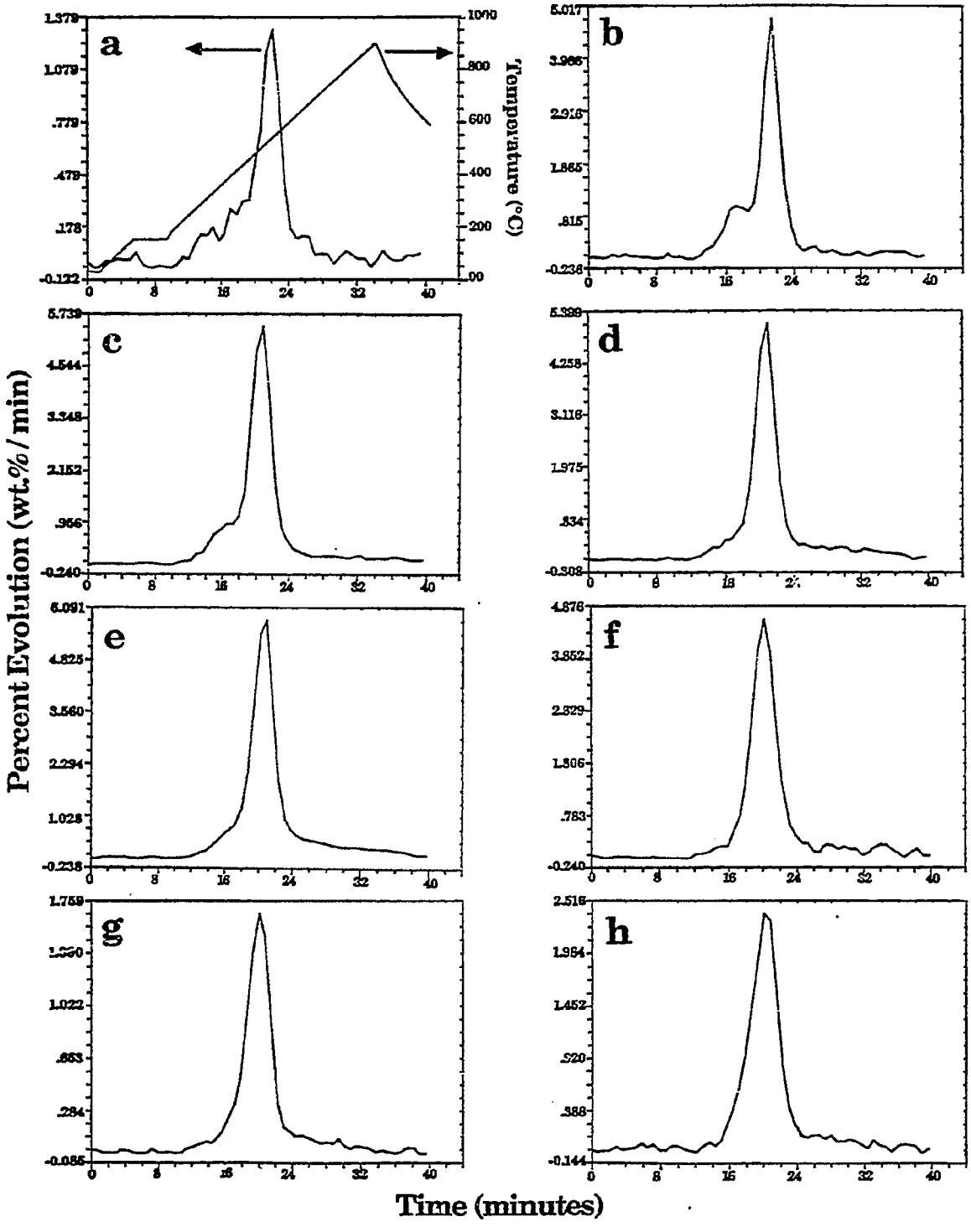

Figure II.A-10. Evolution Rate for Tars/Aliphatic from the Eight Argonne Coals in a TG-FTIR at 0.5°C/s. a) Pocahontas; b) Upper Freeport; c) Pittsburgh; d) Upper Knawha; e) Utah Blind Canyon; f) Illinois No. 6; g) Wyodak; h) Zap.

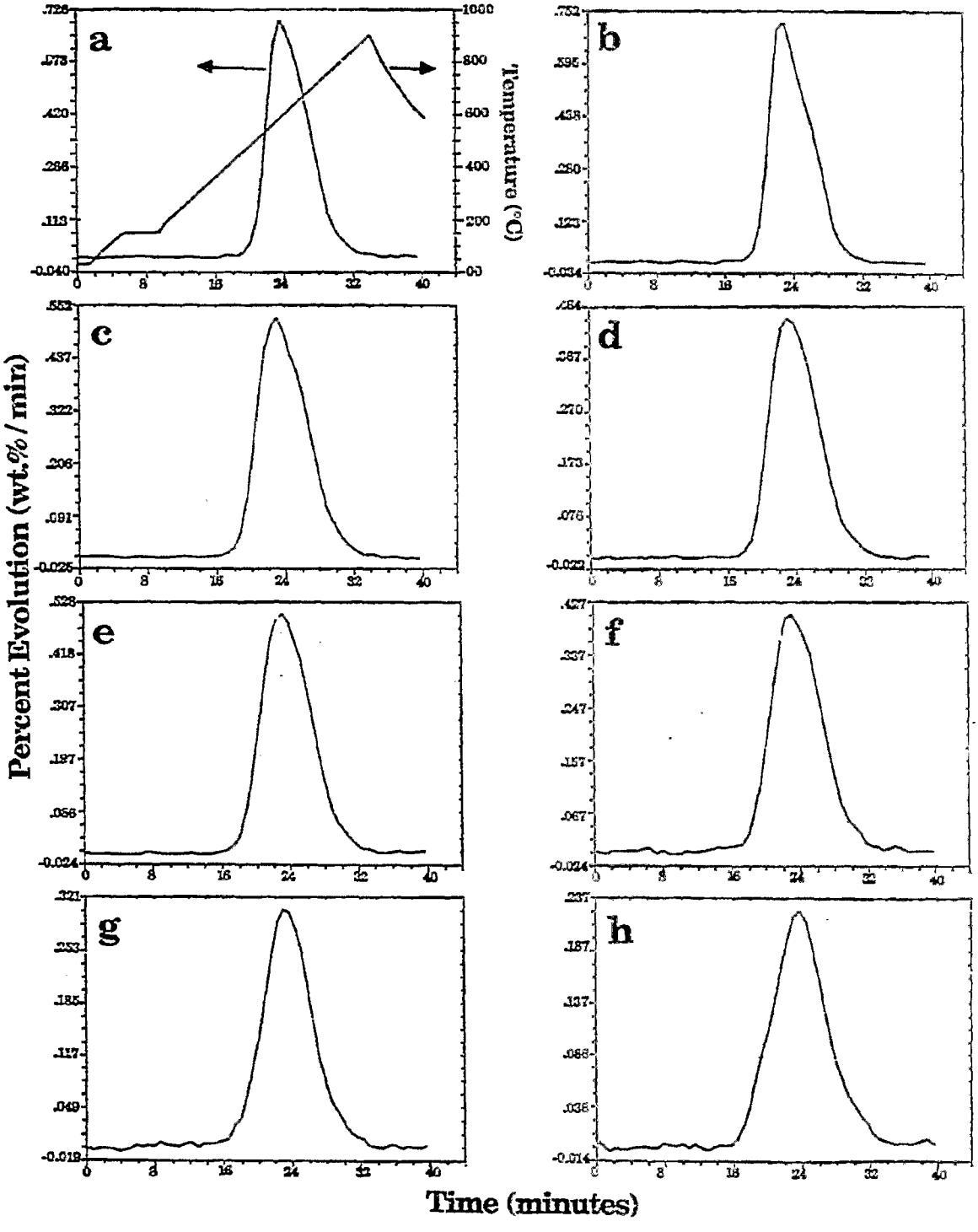

Figure II.A-11. Evolution Rate for CH_4 from the Eight Argonne Coals in a TG-FTIR at 0.5°C/s. a) Pocahontas; b) Upper Freeport; c) Pittsburgh; d) Upper Knawha; e) Utah Blind Canyon; f) Illinois No. 6; g) Wyodak; h) Zap.

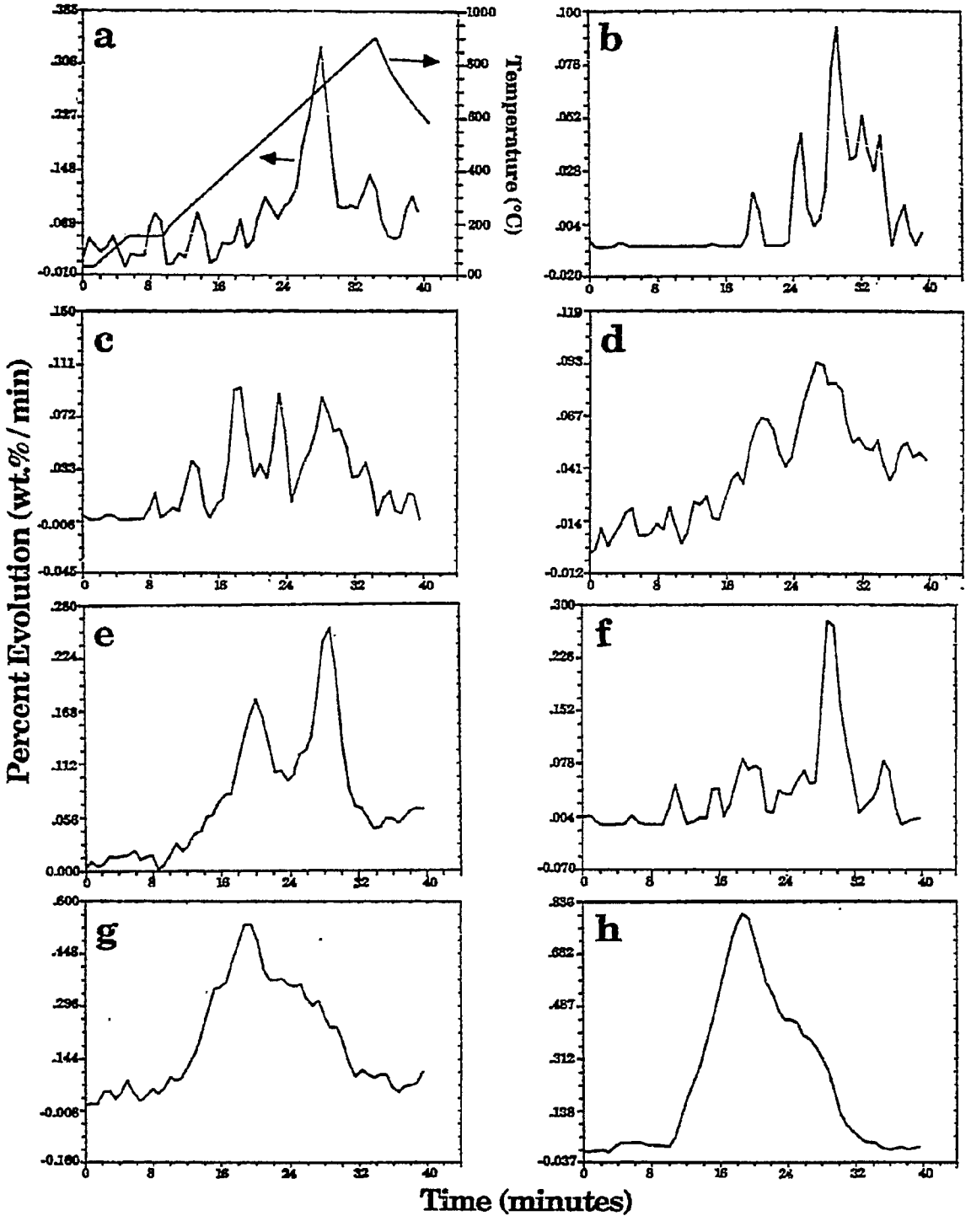

Figure II.A-12. Evolution Rate for CO_2 from the Eight Argonne Coals in a TG-FTIR at 0.5°C/s. a) Pocahontas; b) Upper Freeport; c) Pittsburgh; d) Upper Knawha; e) Utah Blind Canyon; f) Illinois No. 6; g) Wyodak; h) Zap.

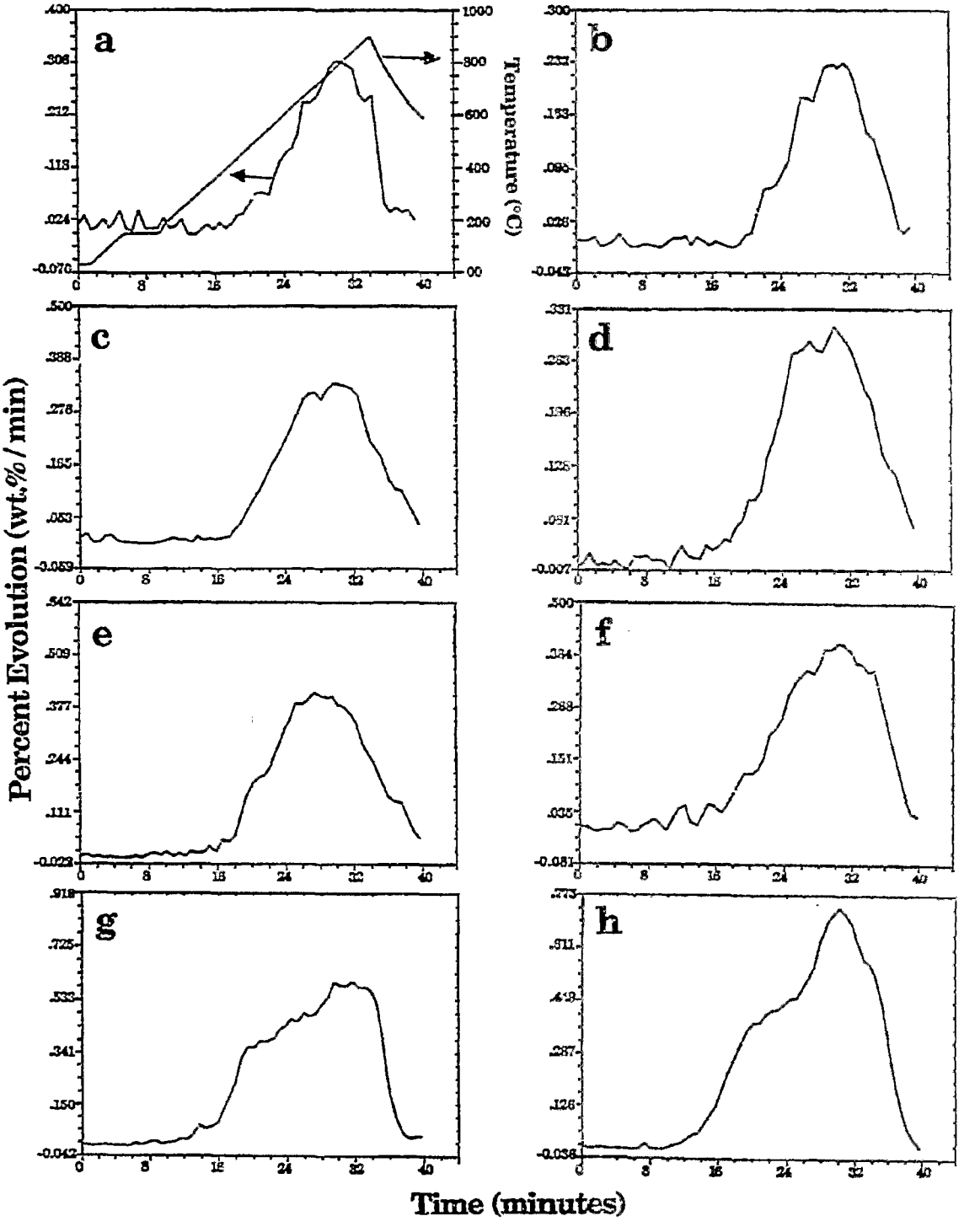

Figure II.A-13. Evolution Rate for CO from the Eight Argonne Coals in a TG-FTIR at 0.5°C/s. a) Pocahontas; b) Upper Freeport; c) Pittsburgh; d) Upper Knawha; e) Utah Blind Canyon; f) Illinois No. 6; g) Wyodak; h) Zap.

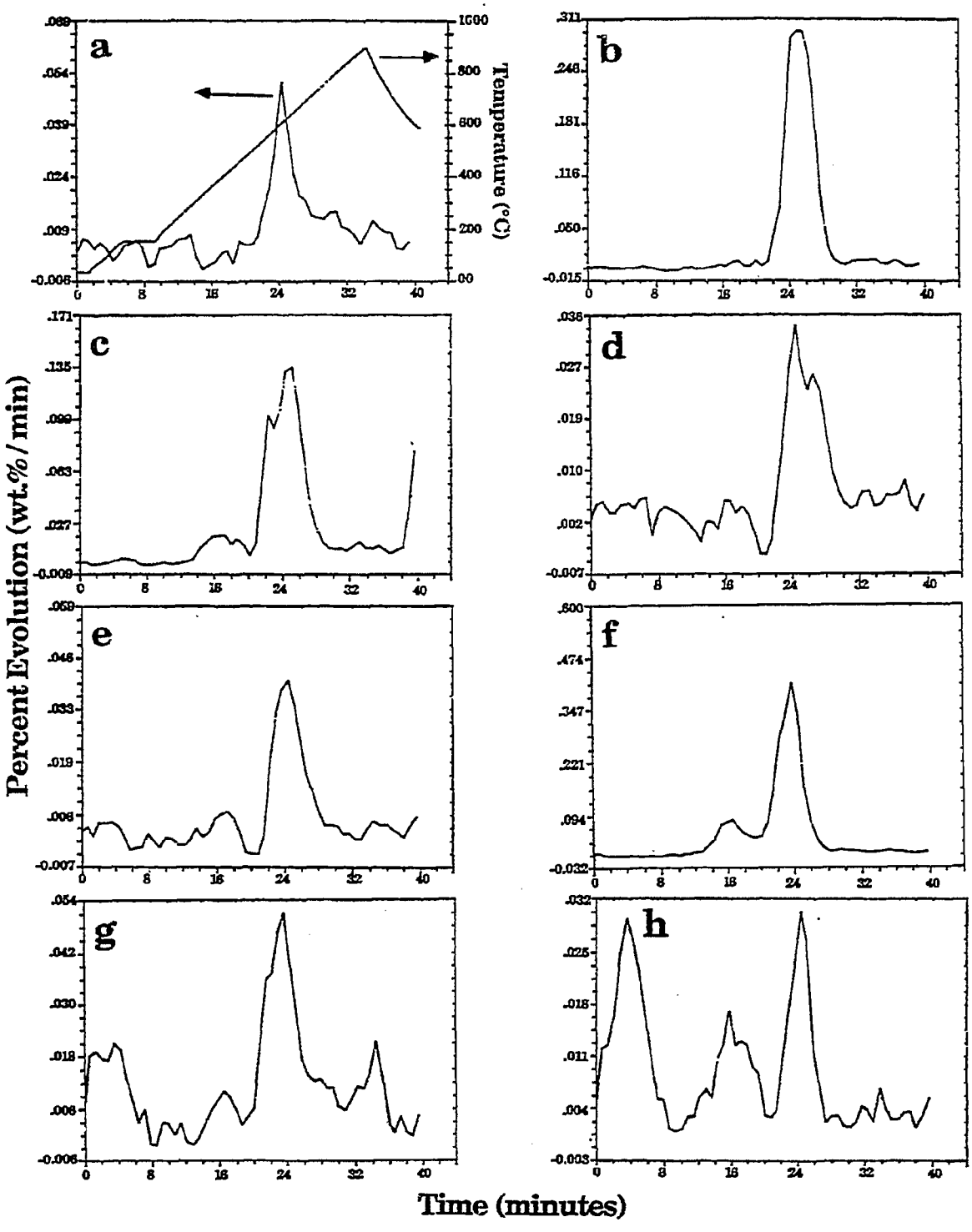

Figure II.A-14. Evolution Rate for SO_2 from the Eight Argonne Coals in a TG-FTIR at 0.5°C/s. a) Pocahontas; b) Upper Freeport; c) Pittsburgh; d) Upper Knawha; e) Utah Blind Canyon; f) Illinois No. 6; g) Wyodak; h) Zap.

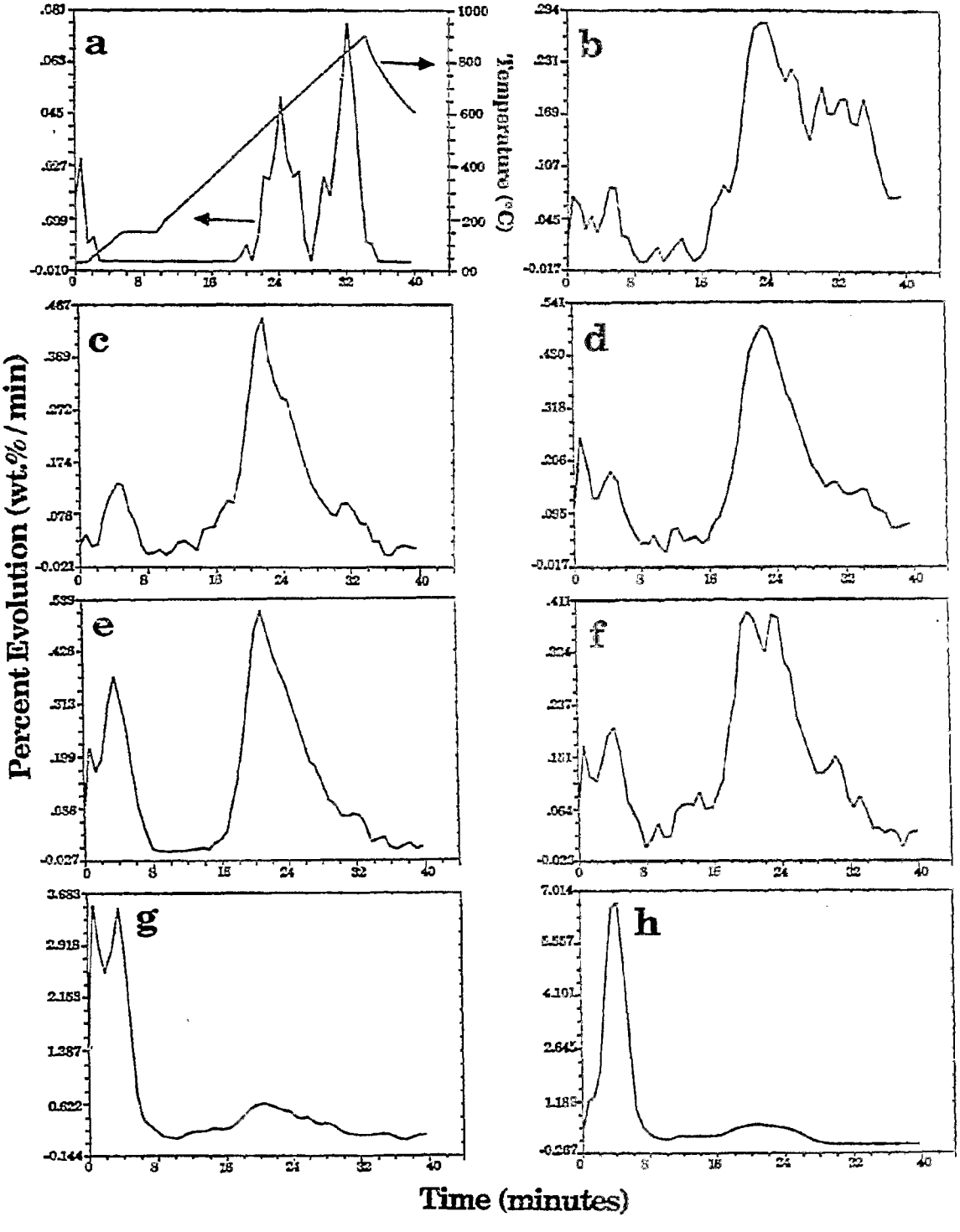

Figure II.A-15. Evolution Rate for H_2O from the Eight Argonne Coals in a TG-FTIR at 0.5°C/s. a) Pocahontas; b) Upper Freeport; c) Pittsburgh; d) Upper Knawha; e) Utah Blind Canyon; f) Illinois No. 6; g) Wyodak; h) Zap.

TABLE II.A-3

ELEMENTAL ANALYSES OF ARGONNE PREMIUM COAL SAMPLES (1)

		%daf basis				% dry basis
		C	H	O	S	Ash
1.	Pocahontas	91	4.7	3	0.9	5
2.	Upper Freeport	87	5.5	4	2.8	13
3.	Pittsburgh #8	83	5.8	8	1.6	9
4.	Upper Kanawha	81	5.5	11	0.6	20
5.	Utah Blind Canyon	79	6.0	13	0.5	5
6.	Illinois No. 6	77	5.7	10	5.4	16
7.	Wyodak	74	5.1	19	0.5	8
8.	Beulah-Zap	73	5.3	21	0.8	6

temperature vicinity for each coal. The results of this analysis are tabulated in Table II.A-4.

In general, the standard deviations are greatest for oxygenated gases (CO_2, CO, SO_2, H_2O) compared to hydrocarbon gases (CH_4, tar/aliphatics). This phenomena was also observed previously (Solomon and Hamblen, 1983). If one assumes a 50 Kcal/mole activation energy, a range in the peak temperature of 40°C corresponds to roughly a factor of 5 in the rate while a range in the peak temperature of 65°C corresponds to roughly a factor of 10 (Solomon and Hamblen, 1983). It appears that about one-half of the volatile products show a variation of x5 or less, while one-half show a variation of x10 or less.

The conclusion was that, for most species, there is a trend of increasing evolution temperature with increasing rank. However, the variations are small enough that the assumption of rank-insensitive kinetics is a good first approximation for all of the major volatile products.

EFR Experiments

Since the last quarter, two additional coals, 200 x 325 fractions of Montana Rosebud subbituminous and Indian Head Zap lignite, were pyrolyzed in the entrained flow reactor. Due to its high water content, the lignite was vacuum dried at 105°C for two days prior to use, while the subbituminous coal was vacuum dried for 1 hour prior to use, as previously practiced with the Argonne coals. The coal feed rates were maintained between 1.5 to 2.2 g/min with N_2 carrier. Particle residence time was approximately 0.7 seconds with furnace conditions of 700°C and 1100°C for both coals. Gas analyses were performed with the Nicolet 1179 FT-IR gas analyzer and a Hach Series 400 gas chromatograph with FID and TCD detectors.

Additional EFR experiments will be done at 1400°C with these two coals. In addition, runs will be done at 700, 1100, and 1400°C with Illinois No.6 coal (which was recently received) and selected demineralized coals.

FIMS Experiments

FIMS analysis experiments were done on the Zap Lignite and Illinois No. 6 coals. In addition, FIMS analysis of the Pocahantas coal was repeated at a higher temperature (500°C maximum instead of 450°C). A method was developed for reading the raw FIMS data obtained from SRI International directly into the SUN 3/260

TABLE II.A-4

Comparison of Temperatures for Maximum Evolution Rate for Volatile Products from Pyrolysis of the Argonne Premium Coals

SPECIES	PEAK #	POCAHONTAS	UPPER FREEPORT	PITTSBURGH	UPPER KNAWHA	UTAH	ILLINOIS	WYODAK	ZAP	AVERAGE
SO_2	1	-	-	375	375	375	360	360	330	363 ± 20
CO_2	1	-	435	420	465	465	435	435	420	439 ± 19
CO	1	495	525	-	465	465	450	435	465	470 ± 30
Tar/ Aliphatics	1	525	510	485	485	485	470	465	465	485 ± 22
H_2O	1	585	555	510	525	495	525	495	495	525 ± 32
CH_4	1	570	555	555	555	555	555	555	570	560 ± 7
SO_2	2	600	615	615	600	615	585	570	600	600 ± 16
CO_2	2	705	750	705	660	735	735	690	615	700 ± 45
CO	2	780	795	795	765	705	780	795	765	773 ± 30
H_2O	2	815	840	795	795	825	765	-	-	807 ± 28

computer on which the FG-DVC model simulations are done. This allows an easier comparison between experiment and theory. These comparisons will be shown in the next quarterly report.

Modeling

The modeling effort was very active during the past quarter. Improvements were made to the FG-DVC model and it was used to model pyrolysis data from the various reactors. Work was also done on comparing the FG-DVC model to the statistical model of Pugmire and Grant. Finally, work resumed on the viscosity model.

FG-DVC Model

Work continued on using the FG-DVC model to model the baseline pyrolysis data obtained for the ten coals from the EFR and TG-FTIR reactors, as well as from FIMS analysis at SRI International. Some of these comparisons will be shown in the next quarterly report. It was also decided to simulate literature data on Pittsburgh Seam coal, since a lot of work has been done on this coal. This will be especially valuable for validating the treatment of internal and external transport effects in the model (see below). In addition, information was obtained from the University of Utah on characterization studies of the Argonne coals by NMR and pyridine extraction. This information was used to calculate parameters needed as inputs into the FG-DVC model.

A lot of work was done on studying the treatment of internal and external transport in the FG-DVC model during the past month. In addition, a sensitivity analysis was done on the various model parameters. Finally, the ability of the model to predict yield variations with heating rate for a bituminous coal was demonstrated. These efforts were undertaken partly to respond to reviewers comments made on the paper "A General Model of Coal Devolatilization" submitted to **Energy and Fuel**. A revised version of the paper was accepted and is included as Appendix A.

In the case of the mass transport effects, it was decided that if the resistances were in series, the internal transport term was dominant in all of the cases that were studied and the external transport term was not needed. We also considered treating the resistances in parallel. However, in this case the surface

concentration of tar needed for the external transport equation cannot be readily calculated. For this reason, and because the assumed (convective) mode of internal transport provides for transport out of the particle, it was decided to drop the external transport term for the time being. However, it is recognized that this may be needed for small particles.

The results of the sensitivity analysis can be summarized as follows. The model has eight coal structure parameters which must be determined for each coal from selected laboratory experiments. Once determined, these remain fixed for all experiments. The model also contains one adjustable parameter, ΔP, the internal pressure difference which drives the volatiles out of the particle. A sensitivity analysis shows that the volatile yield is most sensitive to the fraction of labile bridges, W_B, the crosslinking efficiency parameters $m(CO_2)$ and $m(CH_4)$, and, in some cases (low rank coals, low pressure), to ΔP. The monomer molecular weight distribution parameters, M_{avg} and Δ, have only a weak effect on yields and tar molecular weight distributions. The initial molecular weight between crosslinks, M_C, and the initial oligomer length, ℓ, affect the coal's solvent swelling ratio and extract yield but have little effect on the subsequent pyrolysis behavior.

Work began on comparing the FG-DVC model to the statistical model of Pugmire and Grant at the University of Utah, which is based on percolation theory. The Utah model does not contain the transport or chemistry which we believe are relevant. The percolation theory, however, has some advantages in terms of computational efficiency when compared to the Monte Carlo method used in the FG-DVC model. We are considering ways to combine the FT-DVC chemistry and transport description with the percolation theory mathematics.

Viscosity Model

In the First Annual Report, a semi-empirical predictive model for the viscosity of heated coal was described. The model was to be the same as that published by van Krevelen for linear polymers (van Krevelen, 1976), and included dependencies on functional group composition, average molecular weight, temperature, and chain length, amongst other features. The data used to compare with the model was that of Fong (1986). van Krevelen's model, without adjustable parameters, gave values of viscosity too low by about four orders of magnitude. The major part of this discrepancy is now attributed to the application of a model established for **linear chain** polymers, to a situation in which **crosslinking** undoubtedly plays a major part. Nevertheless, there are features of van Krevelen's

model which appear to have application to a broader array of fluids than molten linear chain polymers, and these will be retained. Specifically, the functional group, average molecular weight and temperature dependence features of van Krevelen's model will be retained, while introducing one parameter to account for the "coalness" of the fluid. A value of that parameter has been established from comparisons of the results of model calculations with the experimental results of Fong, and it will be determined whether the new model can describe results from our own measurements.

Our initial measurements are not direct measurements of viscosity, but of char form and structure. An analysis which will provide relationships between these observations and viscosity is being performed.

The results of some earlier work on cenosphere swelling (Solomon, et al., 1983) are briefly reviewed here. In that research, a single bubble was considered, a cenosphere, under the influence of the contracting force of surface tension and the expanding force due to the pressure difference between the inside and outside of the cenosphere. The pressure difference arises from gas evolution from the pyrolyzing coal fluid, this gas being apportioned between inside and outside in the ratio of the corresponding surface areas. Gas diffusion from inside to outside of the cenosphere is also taken into account.

The above forces act against the resistance of viscosity, as described by Chiou and Levine (1978), giving rise to the following expression for the rate of change of the external radius of the cenosphere, r_2.

$$dr_2/dt = \frac{r_1^3 r_2 (\Delta P_t)}{4\eta (r_2^3 - r_1^3)} \qquad (1)$$

where r_1 is the internal radius of the cenosphere, η is the viscosity, and ΔP_t is the effective outward pressure difference across the cenosphere wall, consisting of surface tension and real differential pressure as described above.

$$\Delta P_t = \frac{n_t RT}{(4\pi/3) r_1^3} - \sigma(1/r_1 + 1/r_2) \qquad (2)$$

where n_t is the total excess tar and gas within the cenosphere, R is the gas constant, T absolute temperature, and σ is the surface tension.

For moderate heating rates of coal, it is believed that there is a fairly well defined sequence of events during pyrolysis. Early in pyrolysis, hydrogen bonds are broken and melting occurs, before appreciable tar evolution. At this stage of development, surface tension is the dominant "active" (i.e., non-resistive) force, leading to the sealing off of larger pores, and tends to collapse these cavities. Surface tension is a classical force associated with a continuous medium, and so is not the appropriate concept to use to describe the behavior of the smallest cavities in coal. A pore radius of 3000 Å was tentatively adapted as a lower pore radius for which the concepts of Eqs. 1 and 2 are valid. Smaller pores will still tend to contract under the influence of intermolecular forces, but steric hindrances will begin to dominate the behavior of the system when only a few macromolecules fit around the "circumference" of a pore. Specifically, the behavior of the macropores (d_4) described by Suuberg (1987) should be described by Eqs. 1 and 2. In the model of Gavalas and Wilks (1980) there is a density of about one d_4 pore per square 10 μm by 10 μm area. This is of the order of the cavity density observed in our SEM measurements. An estimate of the minimum viscosity seen by the coal in this early stage can be obtained by the following analysis, which will be made more precise in computer simulations.

One assumes an early epoch in pyrolysis, when fluidity is established, but before appreciable gas and tar have been evolved. In Eq. 2, let $n_t \rightarrow 0$, and take the internal wall radius, r_1, to be much less than the outer radius, r_2. One can rearrange Eq. 1, and integrate to find that bubbles of initial radius r_1 will vanish as a rate

$$dr_1/dt = \sigma /4\eta \qquad (3)$$

where t is the period for which the coal has a viscosity η , and a surface tension σ . One would count the frequency of occurrence of cavities of different radii in chars treated at different temperatures and time. From this data it should be possible to estimate η from Eq. 3. Empirically predicted values of σ will be used in the computer simulations.

A second test of the viscosity calls for the incorporation of calculated values of the viscosity, η , in Eq. 1, in model simulations of single cell cenosphere swelling, as we now describe. When particles have experienced more extensive pyrolysis at sufficiently high temperatures, evolved tars can cause expansion. The subsequent swelling of the single cell cenosphere is described by Eq. 1. In practice, values of viscosity from the model will be inserted into

Eq. 1, and predicted swelling compared with observed particle swelling. The case of multi-cell particles will be treated in future work.

Our recent experiments on particle heating were described in this and the previous quarter. Calculations have been performed of temperature histories for particles falling through the drop tube furnace, on the assumption of non-swelling (i.e., constant terminal velocity). The particle heats up to the ambient temperature in less than 0.1 sec, while the transit time through the furnace is about 2 sec.

To date, simulations at AFR have been based on average particle properties. As described above, when we take scanning electron microscope (SEM) photographs of a collection of pulverized coal particles it is primarily individual macerals that we see. These macerals have very different swelling histories, so it would be difficult, at best, to try to describe these by one "average" model. In the first simulations of the fluid properties of these particles, parameters derived from TG-FTIR experiments on differentiated macerals will be used.

It is with these results and comparisons that the model parameters established from Fong's viscosity data will be tested against our own results. It is believed that these comparisons will provide a good test for the earlier stages of pyrolysis, including swelling. However, as the experiments stand, they do not give information about the viscosity in the later stages of pyrolysis, when crosslinking is the dominating factor. This problem will be addressed in the next quarter.

Plans

The study of SEM photographs of Pittsburgh Seam coal chars will be continued. This will provide information to help validate the viscosity model. The FG-DVC model will be used to simulate results from baseline pyrolysis experiments with the ten coals. An analysis of pyrolysis data on the Pittsburgh Seam bituminous coal will begin. The work on comparing the FG-DVC model to other pyrolysis models will continue. The EFR experiments with remaining coals should be completed. The studies on cation effects on char reactivity will continue.

II.B. SUBTASK 2.B. - FUNDAMENTAL HIGH-PRESSURE REACTION RATE DATA

Senior Investigators - Geoffrey J. Germane and Angus U. Blackham
Brigham Young University
Provo, Utah 84602
(801) 378-2355 and 6536

Student Research Assistants - Chuck Monson and Russell Daines

Objectives

The overall objectives of this subtask are 1) to measure and correlate fundamental reaction rate coefficients for pulverized-coal char particles as a function of char burnout in oxygen at high temperature and pressure and 2) to provide fundamental kinetic rate measurements of sulfur species with sorbents for a range of stoichiometries under laminar, high-pressure conditions.

Specific objectives for the last quarter include:

1. Continue reactor fabrication and construction
2. Continue preparation of the test cell to house the reactor and the optical instrumentation.
3. Continue preparation and analysis of test samples of char from Utah bituminous coal under atmospheric and greater than atmospheric pressure.
4. Continue development of the sorbent capture test plan.

Accomplishments

Four components of this subtask have been identified to accomplish the overall objectives outlined above: 1) char preparation at high temperature and high pressure, 2) determination of the kinetics of char-oxygen reactions at high pressure, 3) design and construction of a laminar-flow, high-pressure, controlled-profile (HPCP) reactor, and 4) measurements of fundamental sulfur capture rates by sorbents. Most of the effort during this reporting period was focused on components 1 and 3 in preparation for accomplishing the work identified by components 2 and 4.

Component 1 - Char Preparation at High Temperature and High Pressure

The main objective of this component of the study is to prepare chars by three different methods. A simple hot-tube reactor has been employed at atmospheric pressure, and modifications to this reactor will enable char preparation at elevated pressures. The two other reactors from which char samples will be obtained are the BYU high-pressure, entrained-flow gasifier and the HPCP reactor being fabricated for this subtask. Char samples from the three reactors will be compared and their properties correlated with the oxidation kinetics of these chars which will be determined in the HPCP reactor. The reference char sample to which other samples will be compared will be prepared in the HPCP reactor at pressures up to 27 atmospheres.

Chars will be prepared from five different coals from the Argonne premium coal sample bank. Utah bituminous, North Dakota lignite, and Wyoming subbituminous are three of the five coals to be studied. The other two coals will be selected in the near future. A Utah bituminous coal, which is similar to but not the same as the Utah coal in the Argonne bank, has been used to prepare char samples. This coal is now in large supply at the BYU Combustion Laboratory. Small char samples of the Utah coal from the Argonne bank will be characterized and compared to the char samples from the BYU Utah coal.

Literature Review - Wells and Smoot (1987) reviewed the preparation methods for chars and determined that to obtain satisfactory char samples for reactivity testing, the parent coals must be pyrolyzed in a reproducible manner. They also listed six criteria thought to be important to the selection of a pyrolysis method for char preparation. These included heating rate, maximum temperature, residence time, particle size, pressure, and gas composition. A study by Goetz et al. (1982) is quoted by Wells and Smoot (1987) in which char is prepared in nitrogen at 1728 K using a drop-tube furnace. They concluded that drop-tube furnaces and flat-flame burners achieve satisfactory heating rates on the order of 10,000 K/s or higher. They also state that the residence time for pyrolysis should be long enough for complete pyrolysis, but not so long that the coal goes through condensation and polymerization. Residence times in the range of 10-70 ms at the temperature of interest are usually adequate.

A recent study of coal char gasification at elevated pressure was conducted by Guo and Zhang (1986). The chars were prepared by devolatilizing coal in nitrogen at 1070 K for 2 hours. The gasification runs were at 29 atm pressure (30 kg/cm^2) at temperatures of 1120-1220 K. The kinetics were determined by having the carrier gas pass through a sample of char contained in a 22 mm tubular reactor in a furnace and measuring the extent of burnout as a function of time. Under these conditions, the char reactivity followed first-order kinetics. Our approach for kinetics measurements will be under entrained-flow conditions rather than the fixed-bed approach used in this study. Another concern is that char should be prepared at temperatures higher than the temperatures at which the reaction rates are measured to avoid further devolatilization of the char.

Technical Approach - The simple hot-tube reactor (described in the 5th Quarterly Report, Solomon et al., 1987) has provided small amounts of char which have been analyzed. The hot-tube method allows for easy changes in the values of heating rate, residence time and temperature. The varied conditions will aid in determining the conditions which will be selected for the high-pressure reactor. The samples were prepared by flowing nitrogen gas down the tube along with the coal. The nitrogen gas enters the tube from two inlets, one below and one above the coal. The bottom stream of gas fluidizes the coal particles while the top stream entrains the particles and carries them into the tube. The char samples were prepared at temperatures from 1413 to 1484 K. The samples used for the oxidation kinetics studies will be prepared at temperatures higher than those used for the kinetics measurements, to avoid further devolatilization of the char in the reactor. The modification to the simple hot-tube reactor for elevated pressures is complete. The feeder and receiver vessels will be contained in small, stainless steel bulbs.

The BYU high-pressure, entrained-flow gasifier allows for collection of large quantities of char. Data from these chars will be compared with the char

samples prepared by the other methods. The high-pressure, controlled-profile reactor will also be used to prepare char at pressures up to 20 atmospheres with careful control of residence time and temperature. These chars will be designated as reference char samples to which the char samples prepared from the other methods will be compared.

Analysis and Measurements - Seven char samples obtained from the simple hot-tube reactor were analyzed along with a sample of the Utah bituminous coal. The residence time for these chars was calculated in the following manner. A temperature profile was measured for various settings of the reactor, which indicated the maximum temperature of the reactor and the length of the reaction zone used for the calculation of the volume in which the coal converted to char. The reaction zone was defined by the plateau of the temperature profile. The residence time is calculated by:

$$t_r = V_{tube}/w_{N2} \qquad \text{(II.B-1)}$$

where V_{tube} is the volume of the reaction zone in the tube and w_{N2} is the volumetric flowrate of the nitrogen gas through the tube. The flowrate was adjusted as the density of the nitrogen gas changed with temperature. The expanded volume of gas flowing through the tube was determined from the maximum temperature of the tube.

A gas expansion coefficient was defined as the ratio of the normal and maximum temperatures. The nitrogen flowrate, w_{N2} , was corrected by multiplying the flowrate with the gas expansion coefficient. The residence time was then calculated according to Eq. II.B-1. Residence times from 6.0 to 86.4 ms and maximum gas temperatures up to 1484 K have been achieved in the simple hot-tube reactor. Carbon and hydrogen measurements for each char sample from this reactor have been determined and are shown in Table II.B-1, which summarizes the status of the char preparation and characterization to date. As the residence time increased, the hydrogen content in the char sample decreased. The trend shows that the coal is being devolatilized in the reactor. Satisfactory char is being prepared by the simple hot-tube reactor and further comparison studies will be made with these chars. No analyses have been performed on the chars obtained from the BYU gasifier.

Component 2 - Kinetics of Char-Oxygen Reactions at High Pressure

No work planned or conducted.

Component 3 - High-Pressure Reactor Design and Fabrication

The primary objectives of this subtask are to prepare char at high temperature and pressure, to determine the kinetics of char-oxygen reactions at high pressure, and to measure fundamental sulfur capture rates by sorbents at high pressure. The high-pressure, controlled-profile (HPCP) reactor will be used to prepare char, conduct char reaction rate experiments, conduct experiments concerning sorbent capture of sulfur species, and produce and collect tars. The reactor will operate at pressures up to 27 atmospheres and temperatures up to 1700 K. Provision is made for adjustment of axial temperature profile; in-situ measurement of particle temperature, diameter, and velocity; direct sampling of particles; and variable reaction tube diameters.

Table II.B-1
CHAR SAMPLE CHARACTERISTICS

Char Preparation Method	Char Prepared	Analysis C	H	N	SEM	N_2 BET
Hot-tube reactor (atm)	Y	Y	Y	N	N	N
" " " (pressure)	N	N	N	N	N	N
BYU Gasifier	Y	N	N	N	N	N
HPCP Reactor	N	N	N	N	N	N

PRELIMINARY RESULTS

Sample	Residence Time	Temperature Range	Amount Coll.	Analysis, % C	H
288-6	28.4 ms	1192-1211°C	0.145 g	77.3	2.23
288-7	41.1 ms	1140-1200°C	0.245 g	81.1	0.42
288-11	53.9 ms	1140-1200°C	0.193 g	81.6	0.32
288-12	35.9 ms	1140-1200°C	0.238 g	84.3	0.23
288-13	25.4 ms	1140-1200°C	0.303 g	81.9	1.59
1	6.05 ms	1192-1211°C	1.308 g	73.4	3.21
2	86.4 ms	1192-1211°C	0.100 g	77.3	0.83
Utah Coal	---	---	---	77.0	4.36
				77.1	5.27
				75.7	5.10

Literature Review - Two papers of interest were recently presented in March, 1988 at the Western States Section of the Combustion Institute. Mitchell (1988) at Sandia National Laboratories in California used a laminar flow furnace to determine the reactivities of pulverized coal at atmospheric pressure. He employed an optical system which uses two-color pyrometry and light intensity to simultaneously determine particle temperature, diameter, and velocity. Waters et al. (1988) also performed work at Sandia using the optical system described above to determine how dimensional irregularity in char would affect the measurement of the kinetic rate. They found that even with these non-spherical particles, the measured kinetic parameters were relatively insensitive to the assumption that the particles were spherical. Saran char, which is highly irregular in shape, was used in a laminar flow furnace to study how measurements of the optical system using irregular char would vary from the results obtained using spherical char. The variation in measured particle temperature increased significantly for the irregular particles, and diameter uncertainty increased by ±15%. This char is probably a worst case situation for particle shape; no coal char which will be used in the present study will likely be as irregular as the Saran char.

A more complete report of Flaxman and Hallett's (1986) flow and particle heating work was obtained. Flow visualization studies were performed to determine if laminar flow was achieved for the reaction tube and burner design that was currently in use. A finite difference computer program, included in the report, was used to determine particle heating and residence time in the furnace. Some of the conclusions reached were that heating rates increased with increased heating of the secondary gas and with increased particle size up to 100 mm, since particle heating was most strongly affected by wall radiation. The mass flowrate of the primary gas had little influence on the heating rate. Also, lowering the coal feed rate decreased the variations in the temperature histories of different-sized particles. One result of the flow visualization studies was that decreasing the size of the injection tube decreased the chance of unstable flow.

Final Reactor Design - Improvements in the wall heater and preheater designs have been made to reduce cost and improve the reliability of the reactor. Figures II.B-1 through II.B-3 show the final configuration of the reactor and preheater. In an earlier design, reactor wall heat was provided by custom-made, circular heating elements. One of these elements was ordered for testing, but it arrived broken. In consultation with a commercial furnace manufacturer, Calvin Stevenson of Deltec, Inc., it was determined that a standard horseshoe shaped heater would be less expensive, more reliable, and could be made to provide nearly even heating of the reaction tube. The new heater configuration is shown in Figure II.B-2. Each heater will lie on a ceramic insulation tray that slides into the reactor to hold the heater in its proper position. The heater surrounds about three-quarters of the reaction tube and a reflective section of the heater tray surrounds the remaining quarter. This section of the tray is made from a mullite fiber insulation with better radiative heat transfer characteristics than the insulation surrounding the heaters. This results in more even radiative heat transfer and, in conjunction with the high conductivity mullite reaction tube, provides more even heating of the reaction tube.

The preheater has been changed from being an integral part of the reactor head to being a separate, bolt-on assembly (see Figure II.B-3). Other changes

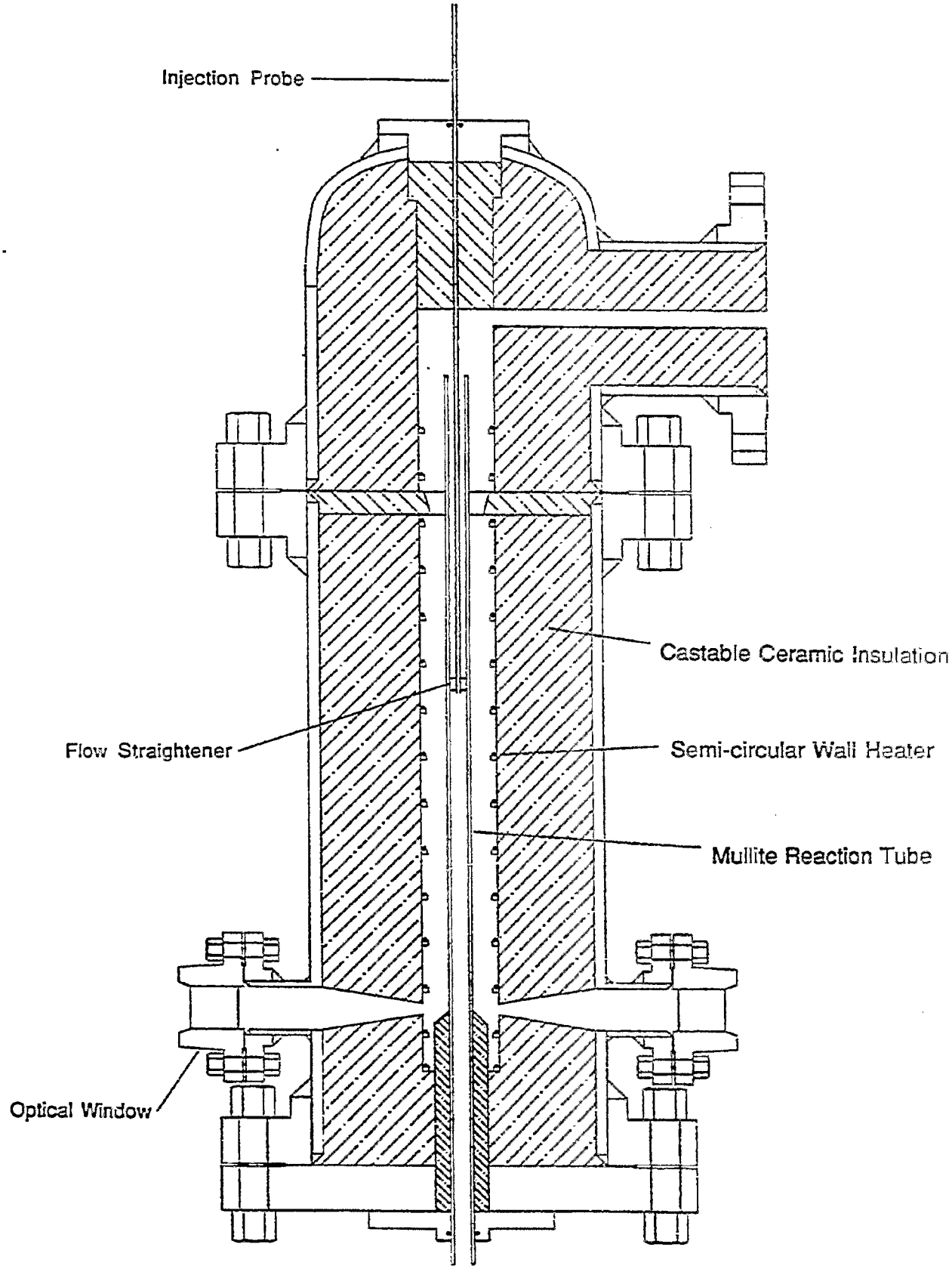

Figure II.B-1. Vertical cross sectional view of reactor.

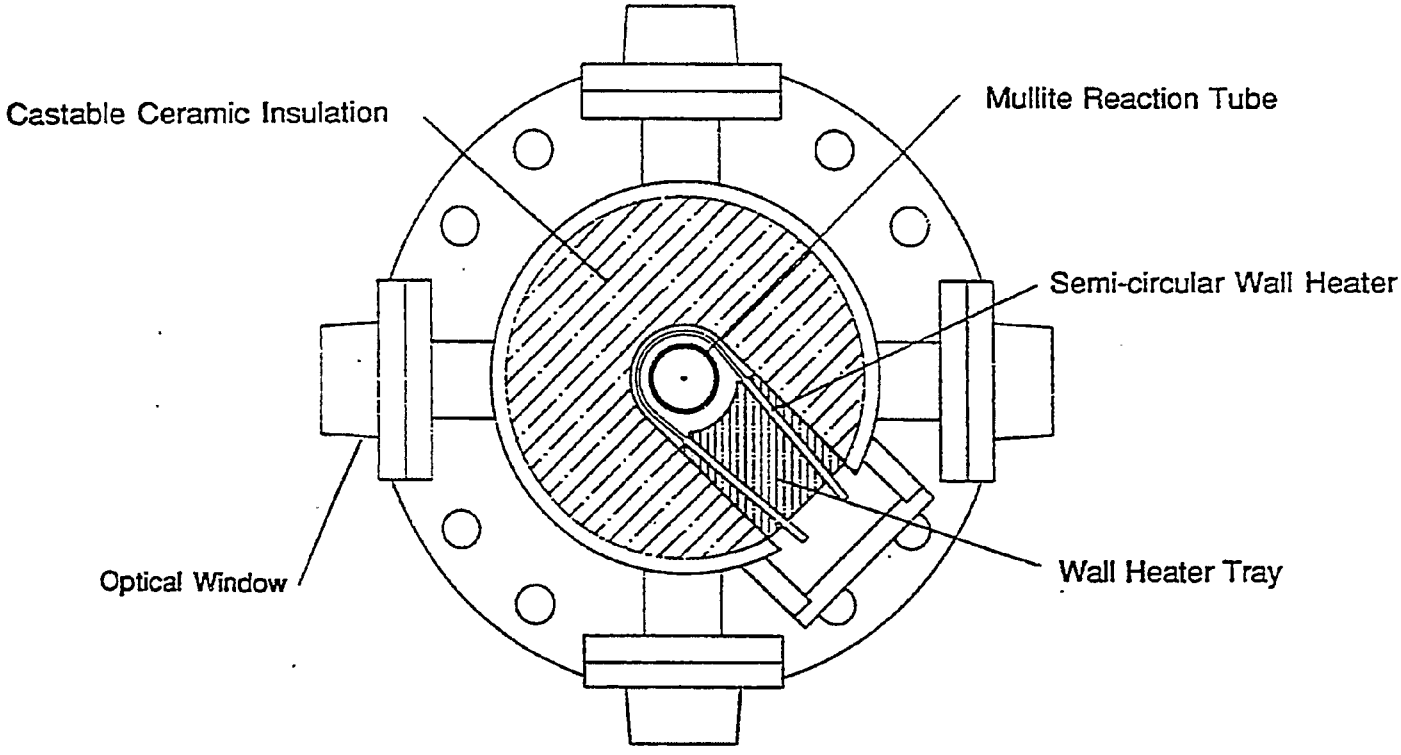

Figure II.B-2. Horizontal cross sectional view of reactor.

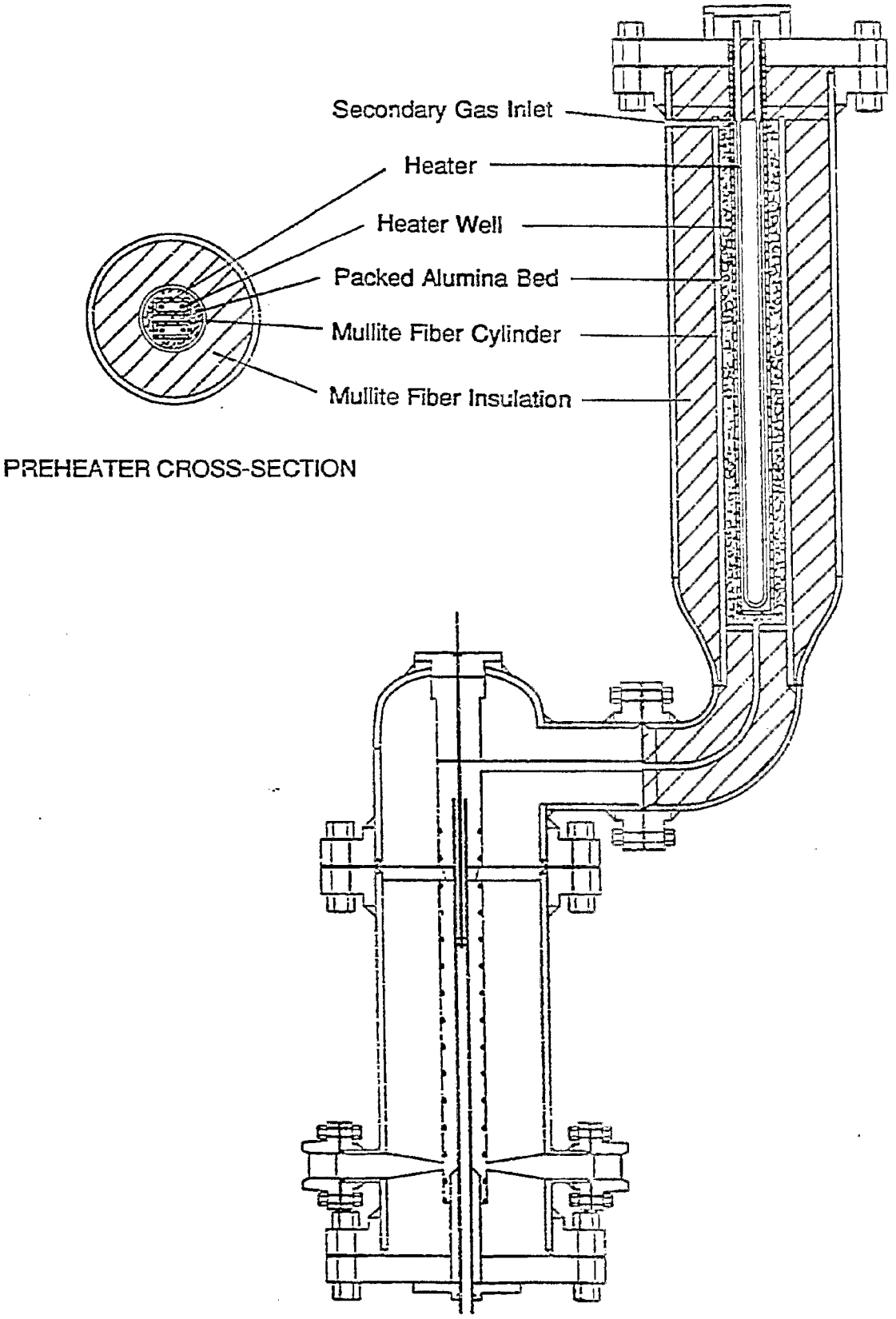

Figure II.B-3. Cross sectional views of preheater.

have been made to increase the longevity of the delicate heating elements. The two heating elements will be enclosed in separate wells that keep the heaters from coming into contact with the packed bed. This bed surrounds the heater wells to ensure good heat transfer. Stress in the heaters will be reduced by allowing them to hang vertically, and the flow area and length of the preheater have been increased to ensure adequate heating of the secondary gas. The packed bed is contained by a mullite fiber cylinder, surrounded by a mullite fiber blanket for additional insulation.

To better account for the variations that will occur in the coal char in the high pressure reactor currently under construction, a method is being investigated that would give more accurate size characterization by making use of two particle dimensions instead of one.

Reactor Testing and Characterization - A program developed to test and characterize the reactor before the char experiments are conducted is outlined below.

Structural Integrity - The vessel will be pressure tested to 1.5 times its maximum pressure at maximum shell temperature. All joints will be checked for proper sealing.

Temperature Profile - A thermocouple will be attached to the end of the injection probe and moved axially through the reaction tube. The preheater and wall heater zone configurations and settings will be adjusted to obtain an isothermal temperature profile for each of the experimental conditions required for the char tests.

Particle Flow - Experiments using the optical system will be conducted to ensure that the particles are fed at a constant rate and that they flow down the centerline of the reaction tube.

Injection Probe - An uncooled injection probe will be used since the char tests will be conducted at temperatures lower than those used to prepare the char. Tests conducted to verify that the char characteristics won't change as a result of heatup in the injector will consist of char injection into an atmosphere of nitrogen only. Since no oxidizer is present in these runs, char properties shouldn't change. The char will be collected and its properties compared with the those determined before the run.

Collection Probe - During the char oxidation experiments, char reactions will be quenched in the collection probe with nitrogen by both cooling and dilution. This quenching process will be tested by making char runs with only nitrogen for both primary and secondary flows and using air as the quench gas. Any change in char characteristics during the run due to oxidation will be a result of improper quenching.

Optical Instrumentation - The optics will be tested using nonfriable carbon spheres (Spherocarb), and the calibration system built into the instrumentation.

Comparison With Other Researchers - Data from atmospheric pressure runs in the reactor will be compared with data obtained by other researchers using similar conditions to establish a baseline. Potential sources are Wells (1985), Solomon et al. (1982), Nsakala et al. (1978), and Kobayashi (1976).

Component 4 - Fundamental Sulfur Capture Experiments

No work planned or conducted.

Other Activities

The research team made a technical review presentation to the AFR management team at Brigham Young University during the reporting period. A member of the research team was invited to present the details of the HPCP reactor design to a regional American Society of Mechanical Engineers' student paper contest in Phoenix, Arizona.

Plans

Further characterization by SEM and N_2 BET will be made in the next quarter on the char samples already obtained. The transition from preparing char samples at atmospheric pressure to elevated pressures will be attempted in the next quarter. Also, chars will be prepared at temperatures up to 1750 K. These chars, as well as two char samples obtained from the BYU Gasifier, will be analyzed by the following methods: CHN determination, Scanning Electron Micrographs, N_2 BET surface area, and particle size measurements. The chars prepared at elevated pressures will have residence times approximately equal to those at atmospheric pressure. This will enable comparisons to be made about the effects of heating rate, pressure, and residence time on the characteristics of char.

Fabrication of the reactor and preheater shells is in progress at the BYU Research Machine Shop. Figure II.B-4 shows the construction schedule for the high-pressure reactor. Plans call for the basic reactor to be completed by the end of the next quarter and the instrumentation and support equipment in place during the following quarter. Testing and characterization will be started in August, 1988 and extend into October, 1988, when char testing will begin. Char will be prepared in the high-pressure reactor during and following reactor testing and characterization.

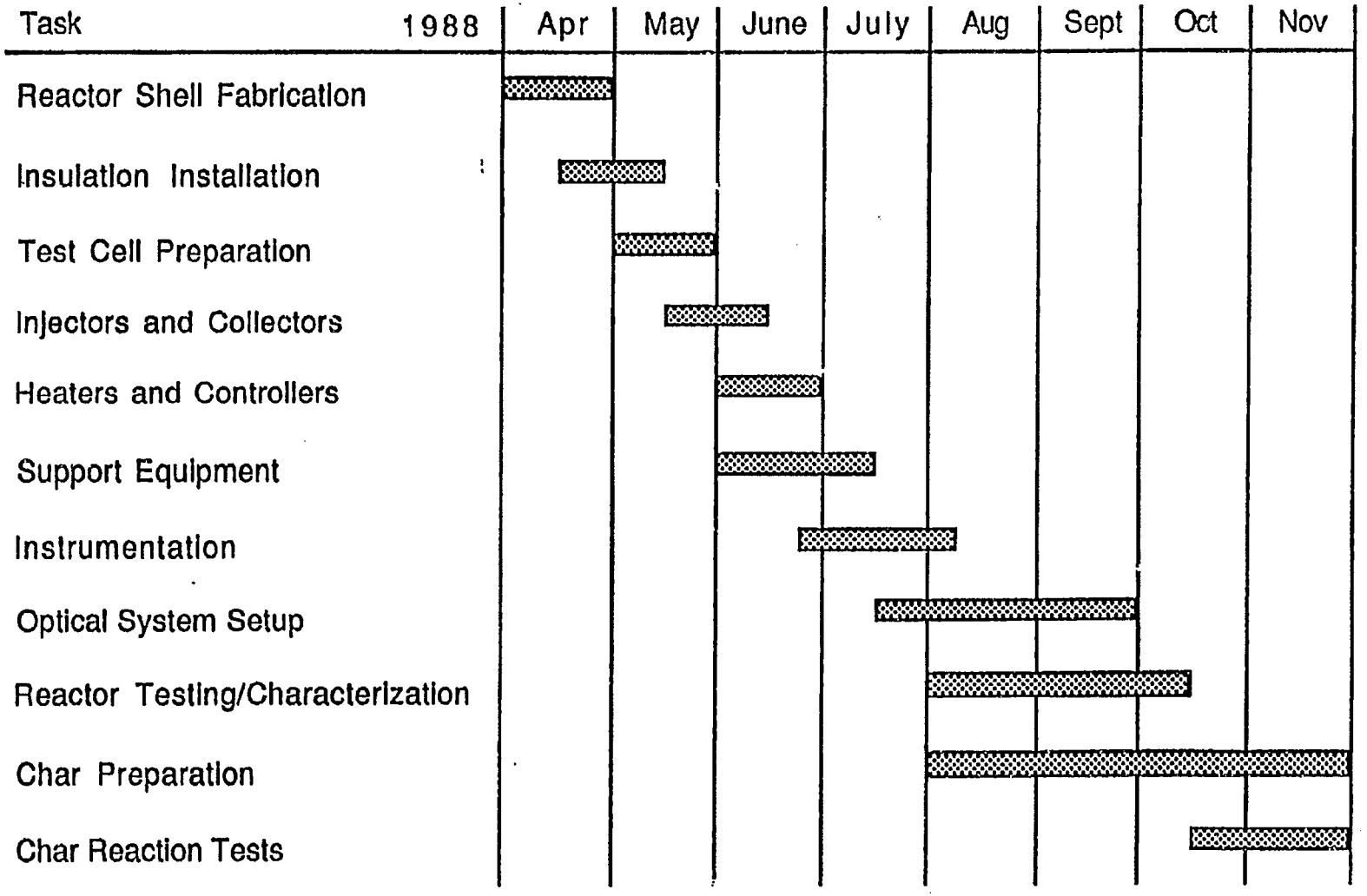

Figure II.B-4. High-pressure reactor construction schedule.

II.C SUBTASK 2.c. - SECONDARY REACTION OF PYROLYSIS PRODUCTS AND CHAR BURNOUT SUBMODEL DEVELOPMENT AND EVALUATION

Senior Investigator - Michael Serio
Advanced Fuel Research, Inc.
87 Church Street, East Hartford, CT 06108
(203) 528-9806

Objective

The objective of this subtask is to develop and evaluate by comparison with laboratory experiments, an integrated and compatible submodel to describe the secondary reactions of volatile pyrolysis products and char burnout during coal conversion processes. Experiments on tar cracking, soot formation, tar/gas reactions, char burnout, sulfur capture, and ignition will be performed during Phase I to allow validation of submodels in Phase II.

Accomplishments

Data collection was temporarily suspended in the TWR as the spectrometer was needed for a different project.

Plans

Continue data collection in TWR for ignition and burnout experiments with chars, coals and demineralized coals.

II.D. SUBTASK 2.d - ASH PHYSICS AND CHEMISTRY SUBMODEL

Senior Investigator - James Markham
Advanced Fuel Research, Inc.
87 Church Street, East Hartford, CT 06108
(203) 528-906

Objective

The objective of this task is to develop and validate, by comparison with laboratory experiments, an integrated and compatible submodel to describe the ash physics and chemistry during coal conversion processes. AFR will provide the submodel to BYU together with assistance for its implementation into the BYU PCGC-2 comprehensive code.

To accomplish the overall objective, the following specific objectives are: 1) to develop an understanding of the mineral matter phase transformation during ashing and slagging in coal conversion; 2) To investigate the catalytic effect of mineral matter on coal conversion processes. Emphasis during Phase I will be on the acquisition of data which will be utilized for model development in Phase II. Data acquisition will be focused on: 1) design and implementation of an ash sample collection system; 2) developing methods for mineral characterization in ash particles; 3) developing methods for studying the catalytic effect of minerals on coal gasification.

Mineral matter in coal is a source for slagging and deposits on reactor or down stream component walls, causing corrosion of equipment. Minerals can also catalyze reactions or can poison processing catalysts. The objective of this research is for the development of a model for the prediction of ash behavior and the correlation of the behavior with the original chemical composition, particle size, physical properties of the minerals and the process conditions. A model will also be developed to predict the catalytic effect of minerals on coal conversion.

Accomplishments

During this quarter, SEM/dispersive x-ray analysis was performed on individual ash spheres that were recovered from the eight stages of the cascade impactor for an "in stack" ash collection from 200 x 325 mesh Zap lignite. As noted in the

Fifth Quarterly Report for this program, the small spheres (< 10 μm in diameter) apparently are shed from the coal particles during the combustion process and contain inorganic components that are intrinsic to the coal. X-ray analysis was performed on the eight size fractionated samples to see if the inorganic species present were biased towards certain particle sizes.

For presumably pure mineral oxides, however, the x-ray data produced consisted of unusually low ash values: typically < 4% total ash. Investigation has led us to believe that due to the small particle sizes and the relatively high acceleration voltage (30 kv) used for the analysis, transmission and sidescatter of the penetrating electron beam through and out of the particles has become significant. This condition would result in x-rays being emitted by the substrate, a graphite layer, that has an atomic number too low for detection on our instrument and would result in the observed low material balance.

To correct for this condition, we will turn down the electron beam acceleration voltage, and also analyze some pure oxide standards in the same particle size range to better calibrate the instrument.

Ash Collection

Two experimental difficulties with the "in stack" ash collection process have been identified, both deriving from the geometry of the TWR. Due to the combination of coal flame, hot gas stream, and shielding room air, positioning the inlet to the Anderson cascade impactor in the stack and ensuring an isokinetic collection flow is a problem. Also, as shown in the previous quarterly report for this program, the time necessary to collect a reasonable amount of ash can be up to 20 minutes, which is unreasonable in respect to the amount of coal fed (~40 g) and maintaining the TWR at an equilibrium operating temperature. To overcome these problems, ash collection tests will be performed in the entrained flow reactor (EFR) with all of the air and ash particles exiting the reactor and flowing through the cascade impactor. This should minimize collection time and ensure a uniform collection.

Plans

Continue collection and characterization of ash particles produced from combustion of different coal types.

II.E. SUBTASK 2.e. - LARGE PARTICLE SUBMODELS

Senior Investigator - Michael A. Serio
Advanced Fuel Research, Inc.
87 Church Street
East Hartford, CT 06108
(203) 528-9806

Objective

The objectives of this task are to develop or adapt advanced physics and chemistry submodels for the reactions of large coal particles (> 0.5 mm) and to validate the submodels by comparison with laboratory scale experiments. The result will be coal chemistry and physics submodels which can be integrated into the fixed-bed (or moving-bed) gasifier code to be developed by BYU in Subtask 3.b. Consequently, this task will be closely coordinated with Subtask 3.b.

Accomplishments

The design of the fixed-bed reactor was completed, parts were ordered and construction began. This reactor will have on-line analysis of evolved volatile products, functional group composition and particle temperature.

Design and Construction of Fixed-Bed Reactor

Additional modifications were made to the design for the fixed-bed reactor, as described below. A revised schematic of the main reactor section is given in Fig. II.E-1.

The reactor includes both inner (5) and outer (8) quartz tubes and a quartz gas preheat section (1). Quartz is used to withstand the high heat load and minimize background radiation. A second heater (2) will be put inside the outside reactor tube to provide an additional heat source, if necessary. Two water-cooled aluminum flanges provide for securing the reactor system in place. These flanges are screwed together with three spring loaded screws to allow for heat expansion. An O-ring seal (6) is used for the inner tube and teflon gaskets for the outer tube.

The coal sample (0.5 - 3 g) sits on a steel wire mesh in a quartz basket

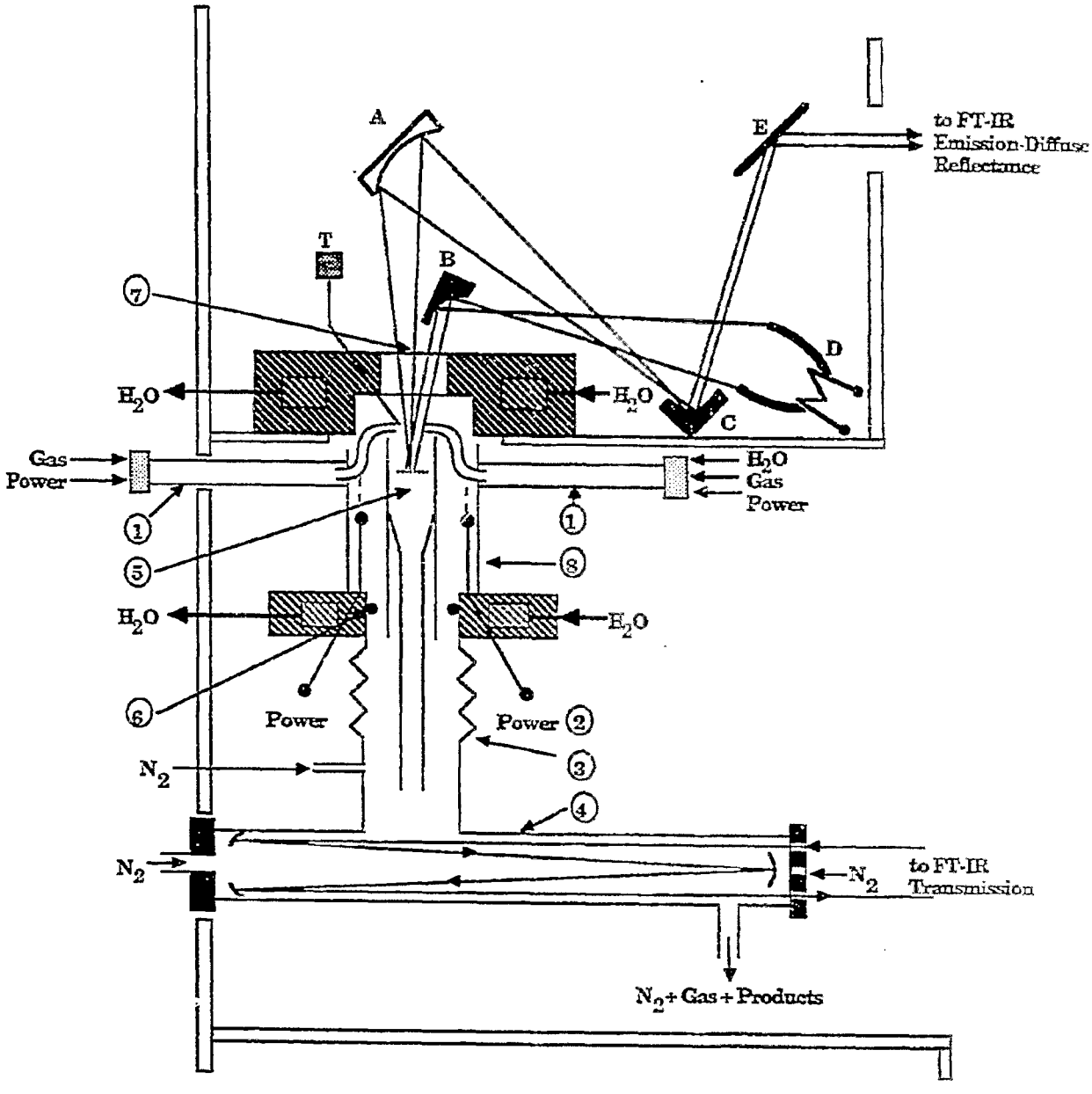

Mirrors

A: 4" Concave Mirror
B, C: Off-axis Parabola Mirrors
D: Ellipsoid Reflector with the IR Source
E: Flat Mirror

T: Thermocouple

1. Gas Preheater, H_2O Evaporator
2. Power to Additional Heater
3. Metal Bellows-Glass Connector
4. Dual Pass Cell
5. Quartz Reactor Tube (I.D. 1.18") with Grid to Hold Coal Sample
6. Vyton O-ring Seal
7. KBr Window
8. Outer Reactor Tube

Figure II.E-1. Revised Schematic of Fixed-Bed Pyrolysis Reactor.

which is kept in place by quartz spikes protruding into the inner reactor tube (5). The sample can be changed through the removable window (7). A thermocouple is placed above the coal surface in a quartz capillary tube. The reaction of additives with the coal surface can also be examined by injecting the reactant through this capillary tube. A bellows (3) allows for an elastic metal glass connection and for relatively trouble-free alignment of the transmittance cell (4).

The difference between most previous experiments of this type and ours is that the diffusely reflected light (DR) is led into the interferometer in the same way as the emitted light (E). Either the E plus DR or E spectrums (the latter with the IR source shut out) can be measured. Then DR = (E + DE) - E can be derived. This arrangement makes it possible to build a more straightforward optical pathway, as well as increase the sensitivity of the DR spectra measurement by increasing the incident light intensity. The IR source is a coil put into the primary focal point of an ellipsoidal reflector (D). The secondary focal point coincides with that of an off-axis paraboloid mirror (B), thus providing a high intensity parallel beam. Reflected light is collected at an angle different from the incident light to minimize the specular reflected light content in the DR spectra. E plus DR light is collimated the same way incident light is, thus providing a relatively simple optical pathway to the FT-IR spectrometer.

Initially, the plan is to use two separate spectrometers. An IBM IR/32 with an IBM PC/AT will be used for the evolved gas analysis (EGA). The PC/AT will also provide the temperature programming and data handling capability developed at AFR for the TG-FTIR instrument. A second spectrometer, either on IBM IR/32 or a Nicolet 20SX, will be used for E, DR measurements.

Plans

Complete construction of fixed-bed reactor. Begin model development for large particle submodel. Consider interface of this model with the BYU fixed-bed model, along with the specific needs for modeling mild gasification processes.

II.F. SUBTASK 2.f. - LARGE CHAR PARTICLE OXIDATION AT HIGH PRESSURES

Senior Investigator - Angus U. Blackham
Combustion Laboratory
Brigham Young University
Provo, Utah 84602
(801) 378-2355

Objective

Provide data for the reaction rates of large char particles of interest to fixed-bed coal gasification systems operating at pressure.

Accomplishments

No work planned.

Plans

No work planned.

II.G. SUBTASK 2.G. - SO_x/NO_x SUBMODEL DEVELOPMENT

Senior Investigators - L. Douglas Smoot and B. Scott Brewster
Brigham Young University
Provo, Utah 84602
(801) 378-4326 and 6240

Graduate Research Assistant - Richard Boardman

Objectives

The objectives of this subtask are 1) to extend an existing pollutant submodel in PCGC-2 for predicting NO_x formation and destruction to include thermal NO, 2) to extend the submodel to include SO_x reactions and SO_x-sorbent reactions (effects of SO_3 nonequilibrium in the gas phase will be considered), and 3) to consider the effects of fuel-rich conditions and high-pressure on sulfur and nitrogen chemistry in pulverized-fuel systems.

Accomplishments

The components of this subtask are 1) extension of an existing pollutant submodel to high pressure and fuel-rich conditions (including thermal NO formation), 2) modification of the current comprehensive code to include sorbent particle injection and reactions (including sulfur capture), and 3) extension of the pollutant submodel to include SOx formation.

Component 1 - NO_x at High-Pressure/Fuel-Rich Conditions

The goal of this subtask is to extend the current pollutant submodel in the comprehensive code to be applicable to high-pressure, fuel-rich conditions such as are common in gasification processes. An important part of this extension is the inclusion of thermal NO formation which may be significant at the higher temperatures typical of gasification in oxygen. The integration into PCGC 2 of a revised NO_x submodel, including thermal NO, was described in the 5th Quarterly Report. With thermal NO turned off, the revised submodel correctly predicted fuel NO. Thermal NO predictions for a swirling, coal-laden reactor, however, turned out to be unreasonable. Consequently, modifications to the theory and calculation method were considered. A review of the literature for modeling turbulent flames is given below. This review will provide a foundation for describing the current direction of the NO_x submodel development.

Theoretical Review - The solution of the major field variables in PCGC-2 is based on the "fast" chemistry assumption where all reactions go to equilibrium as soon as the reactants are mixed. Specification of the local pressure, enthalpy, and elemental composition is sufficient to determine the equilibrium composition, temperature, and fluid density of the gas mixture. For turbulent flames it can be reasonably assumed that all species have equal turbulent diffusion coefficients. Thus, the local elemental composition is determined throughout the system by tracking the mixing of primary gas, secondary gas, and coal offgas. Two conserved scalars, f (primary gas mixture fraction) and h (coal offgas mixture fraction), are used in PCGC-2 to track this mixing. The energy equation is then solved to determine the enthalpy. In summary, with knowledge of the instantaneous values of f, h and enthalpy, the instantaneous

values of species concentrations and temperature are uniquely determined. In other words, the system is dependent exclusively on the state of mixing and the local enthalpy.

For some species, the "fast' chemistry assumption is inappropriate. In such cases, the species are not exactly conserved and cannot be linearly related to the mixture fraction. For instance, the concentrations of radicals are often considerably higher than the equilibrium values in fuel-rich zones. In cases where non-equilibrium effects are important, significant error can result in the predicted temperature if these effects are ignored. In order to account for these effects, a reaction mechanism may be incorporated for the non-equilibrium species. When the extents of these reactions are known, the thermochemical state of the system may be determined. The system, therefore, exists in a state of partial equilibrium, constrained from full equilibrium by imposing necessary reaction mechanisms and their corresponding extents. For each kinetically-limited reaction, a new scalar progress variable, r, is introduced. The value of r varies from zero (unreacted flow) to unity (full equilibrium). The reactive scalar is calculated by casting r in terms of one of the non-equilibrated species and solving a continuity equation for this species with a reaction source term included. The reaction source term is defined by the prescribed reaction mechanism. All concentrations, as well as density, temperature, and all source terms of r, can be formulated as functions of the independent progress variables, r, the mixture fractions, and enthalpy.

Pollutant species typically exist at levels well below their equilibrium values. Since they are usually only present in trace quantities, they are assumed to have negligible influence on the thermochemical state of the system. However, the prediction of kinetic source terms may involve radical concentrations which are themselves out of equilibrium.

An alternative approach to calculating nonequilibrium effects in diffusion flames is the perturbation analysis of Bilger (1978, 1979, 1980). In this approach, species mass fractions are partitioned into an equilibrium value (dependent on the mixture fraction) and a perturbation of this value. Experimental evidence suggests that, over a broad region of a given gas-phase diffusion flame, the molecular species composition is only a function of the local equivalence ratio, even though the products are not in equilibrium. Fenimore and Fraenkel (1981) tested and confirmed this hypothesis for thermal NO concentrations in laminar, gaseous, diffusion flames. This observation suggests that the perturbation factor is a well-conditioned, approximately linear function of the independent variables.

Both the NO_x and SO_x submodels require an adequate description of chemistry/turbulence interactions and efficient and accurate numerical solvers. The chemistry/turbulence interactions have three aspects: 1) the kinetic mechanism, 2) calculation of the instantaneous species concentrations and temperature to be used in the rate equations, and 3) calculation of mean reaction rates for source terms in the species continuity equations. The kinetic mechanisms describing pollutant formation are typically composed of a large number of parallel and sequential steps. These steps may or may not be well-understood. However, from well-designed experiments, it is often possible to develop a sequence of global reactions which contains sufficient detail to describe the overall process for reactors of interest. The global rates should

account for the major actors (species) in the mechanism and be capable of predicting the effects of combustion process variables.

When the rate expressions are dependent on radical species such as hydroxyl molecules and oxygen atoms, these concentrations must be predicted a priori. Various theories have been suggested and tested for the prediction of non-equilibrium radicals in simple H_2-air flames (Janicka and Kollmann, 1982; Bilger, 1980). They each refined the description of the reacting H_2-air system by postulating a set of fast-shuffle reactions to account for species in partial equilibrium. Janicka and Kollmann (1978) modeled the partially equilibrated oxy-hydrogen radical pool using a combined reaction progress variable and mixture fraction progress variable. Bilger (1980) applied his perturbation approach to account for the departure from equilibrium. Correa et al. (1984) and Pope and Correa (1986) included CO in the non-equilibrium pool and predicted the radical concentrations in a turbulent $CO/H_2/N_2$ jet diffusion flame. However, in the rich parts of the flame, there are discrepancies in the calculated CO and OH concentrations. It is yet unclear whether these approaches can be successfully applied to hydrocarbon systems and coal flames. In a separate project, a non-equilibrium CO submodel is being incorporated into PCGC-2 (Colson, 1988). Thus the effects of nonequilibrium in the major species pool are currently being implemented into PCGC-2.

In a study related to the work of Correa and coworkers, Drake et al. (1984, 1987) measured and modeled the formation of superequilibrium radicals and nitric oxide in atmospheric pressure, turbulent diffusion flames. Their model for NO was based on the Zeldovich mechanism which is reduced to a single rate expression involving atomic oxygen. This rate expression is identical to that being implemented into the NO_x submodel to account for thermal NO formation. Using their two-scalar (reaction progress and mixture fraction) model to predict the radical pool, increases in thermal NO were a factor of 1.4 to 2.5 over the values calculated by oxygen radicals taken in equilibrium. This difference is attributed to a large decrease in the system temperature (-250 K) and an increase in the concentration of oxygen radicals.

The effect of turbulence on the mixing of reactants and products can dramatically affect mean chemical kinetic rates that have reaction time scales on the order of the turbulent time scales or less. This includes essentially all gas phase kinetics where the species have finite kinetics. This influence is the result of the random fluctuations of the temperature and species compositions at any given point in time. A method for obtaining mean reaction rates from information provided by the progress variables is possible, provided the instantaneous temperature and species concentrations are unique functions of the instantaneous progress variables. While the combustion models do not solve for the instantaneous values of the progress variables, a statistical distribution of the instantaneous values can be hypothesized. Given the mean value of the progress variable, its variance about the mean and an assumed shape for its distribution, the probability of the instantaneous values can be statistically defined. In other words, a probability density function (pdf) of the instantaneous values is defined by the mean, its variance and the shape of the distribution. Equations for the mean and the variance are easily modeled while experimental and modeling experience has provided information for selecting the shape of the distribution. Typically, a clipped Gaussian shape is selected for the pdf. The mean rates are thus obtained by integrating the instantaneous rates over the statistical probability of the progress variables.

When two progress variables are involved, a double integration is performed over the joint probability function of the progress variables. This method is the same technique that is used to determine the time-mean gas properties, including density, species concentrations, and temperature.

NO_x Submodel Progress - In PCGC-2, the residual enthalpy is defined as the difference between the actual enthalpy (determined from the energy equation) and the adiabatic enthalpy (determined uniquely from f and h). The assumption is made that the sensible heat loss to the surroundings is small relative to the adiabatic enthalpy, and the turbulent fluctuations in the residual enthalpy are neglected. Thus, the instantaneous temperature is uniquely defined by the instantaneous values of f, h, and h_r, but mean reaction rates are calculated for source terms in the NO_x species continuity equations by convolving over the joint probability of only f and h. The formation of fuel NO has been successfully predicted for coal reacting flows using a simple three-reaction mechanism as discussed in the 5th Quarterly Report (Solomon et al., 1987). The global rate expressions for this mechanism involve stable, non-radical species eliminating the need to predict non-equilibrium radical species. Thermal NO formation, on the other hand, is generally agreed to occur through the Zeldovich mechanism, and a single rate equation has been derived for thermal NO which is consistent with the derivations of other investigators. Unfortunately, this rate expression contains the concentration of atomic oxygen radicals which must be accurately calculated. Finally, each of the rate expressions are exponential in temperature and may depend on the existence of superequilibrium, unreacted species in fuel-rich regions of the flame.

In the current theory for the formation of fuel NO, instantaneous species concentrations are obtained assuming the perturbation technique of Bilger is acceptable. The functionality of the linear perturbation factor was discussed in the 5th Quarterly Report (Solomon et al., 1987). Successful prediction of fuel NO has been achieved by this approach for diverse pulverized coal flames. During the past quarter, an attempt was made to jointly predict fuel NO and thermal NO using a similar but redefined perturbation factor. The calculations thus far have been physically unrealistic, and the current method is under investigation.

A new method for calculating the instantaneous species mass fractions has been developed and is being tested. In the new method, the instantaneous factors are determined by solving mass balances for C, H, O, and N at each node for the following set of global reactions:

$$N_2 + O_2 \longrightarrow 2NO$$

$$HCN + O_2 \longrightarrow NO + \ldots\ldots$$

$$NO + HCN \longrightarrow N_2 + \ldots\ldots \qquad \text{(II.G-1)}$$

The four mass balances can be written in terms of three extents of reaction. Additional equations include the species continuity for NO and HCN in terms of their mean reaction rates and the mole fraction constraint. Thus, on each iteration, a system of 7 equations is solved for 7 unknowns to determine the instantaneous species values. A submodel based on the revised NO model has been developed and is currently being debugged and tested.

The extents of reaction represent the departure from equilibrium and, like before, are assumed to depend only on f and h. This assumption is valid provided that the solution of the major field variables is accurate based on the "fast" equilibrium assumption.

Component 2 - Sorbent Particle Chemistry

This subtask component is aimed at developing a sorbent particle submodel for incorporation into PCGC-2. The submodel will include both calcination chemistry and reactions with the gas phase. The submodel will be an extension of independent work being performed by Pershing and coworkers at The University of Utah, where a sorbent chemistry submodel for fuel-lean conditions is being developed and incorporated into PCGC-2. Work has been initiated on this subtask to monitor the project at the The University of Utah. Progress during the last year on the Utah submodel development is described in the Second Annual Report of the Advanced Combustion Engineering Research Center (Smoot et al., 1987) and summarized below.

The objective of the Utah project is to develop a computational procedure which can be used to predict the effectiveness of dry sorbent injection in a variety of combustion applications. The approach is to identify an appropriate sulfation model to describe the CaO/SO_2 reaction system in the furnace environment and to modify PCGC-2 to include the sulfation model and the associated sorbent particle tracking. During the past year, a sulfation model based on a grain formulation with nonlinear SO_2 kinetics and CaO sintering was selected and modified. The model selection was based on good agreement between model predictions and the most recent, time-resolved sulfation data. It was also based on the observed granular nature of CaO particles removed from the reaction zone and the overall simplicity of the model. Figure II.G-1 shows the ability of the grain model to correlate new short-residence-time (less than 200 ms sulfation data of Milne and Pershing,1987). The sulfation rate and loss of surface area due to sintering appear to be more rapid at short residence time than currently assumed, and efforts during the coming year will address these issues.

Component 3 - SO_x Formation

This subtask component will model the gas-phase reactions that generate the sulfur species for input to the sorbent capture model developed under Component 2 of this subtask. A review of the literature is being made to identify recent work related to sulfur pollutants. Objectives include: 1) identifying the steps and kinetics in the SO_x formation process, 2) isolating the most important or rate-determining steps, 3) identifying the dominant products or stable species in combustion gases, 4) determining whether an equilibrium approach is acceptable, 5) gaining a comprehensive understanding of the effect of reactor parameters and operating conditions on the sulfur species, and 6) identifying important SO_x/NO_x interactions. A previous literature review on sulfur pollutants has been useful in reducing the current literature study to only the most recent sulfur studies and journal publications.

Plans are also being made to elucidate some of these issues by measuring sulfur pollutant species as described in Subtask 2.h. Data obtained from independent investigations at the BYU Combustion Laboratory will also be considered. An analytical chemistry group as been formed for the purpose of

correlating the measurements and data reduction for the combustion experiments. Procedures are currently being resolved to measure both SO_2 and SO_3.

The major species of interest in hydrocarbon flames containing sulfur are H_2S, COS, CS_2, SO_2, and SO_3, with SO_2 typically being the dominant product (Kramlich et al., 1984). In fuel-rich flames lacking significant hydrocarbons, H_2S as been shown to be the dominant stable non-SO_2 species. In hydrocarbon flames at richer conditions, COS and CS_2 can replace H_2S as the non-SO_2 product (Nichols, 1986; Kramlich et al., 1984). This list constitutes the pool of species that will be measured during the combustion tests.

Plans

Plans for the next quarter include continuation of the NO_x model development and validation. The new approach involving a system of equations will be tested and evaluated. Predictions will also be made for selected gaseous combustion systems described in the 5th Quarterly Report (Solomon et al., 1987). An evaluation of sulfur species data collected during recent Combustion Laboratory experiments will also be made to begin laying the foundation for the SO_x submodel.

II.H. SUBTASK 2.H. - SO_x/NO_x SUBMODEL EVALUATION

Senior Investigator - Paul O. Hedman
Brigham Young University
Provo, UT 84602
(801) 378-6238

Student Research Assistants - Aaron Huber, David Braithwaite,
Laren Huntsman, and Gregg Shipp

Objectives

The objectives of this subtask are 1) to obtain detailed mixing and turbulence measurements for radial crossjet injection of sorbent particles in a cold-flow facility designed to replicate the geometry of a 2-dimensional, axisymmetric entrained flow coal gasifier, 2) to obtain concentration profile data for sulfur and nitrogen pollutant species from laboratory-scale, coal gasification at atmospheric and elevated pressure with and without sorbents, and 3) to investigate the effect of pressure on the effectiveness of sorbent injection in capturing sulfur pollutants.

Accomplishments

This subtask is being carried out under three subtask components: 1) A cold-flow investigation of sorbent mixing fluid mechanics, 2) modifications of the laboratory-scale reactor to accommodate sorbent particle injection, and 2) space-resolved sulfur and nitrogen pollutant measurements in the laboratory-scale reactor.

Component 1 - Sorbent Mixing Fluid Mechanics

The BYU cold flow facility is being used to simulate the flows that exist in the entrained flow gasifier when sorbent is injected in a flow that is perpendicular to the main gasifier flow. Previous investigators (see Webb and Hedman 1982; Jones, et al., 1984; and Lindsay, et al., 1986) have used the BYU cold-flow facility to simulate the flows that exist in one of the BYU coal combustors and the BYU entrained-flow gasifier. The existing cold-flow facility is being modified to include crossflow jets for sorbent injection. Also, the flow chamber design is being changed from previous studies. The new flow chamber is being made of transparent plastic to simplify making LDA measurements and enable qualitative flow visualization with smoke. Smoke visualization will provide a qualitative means of examining the rate of mixing of the crossflow injection of the sorbent jets.

Modifications to the BYU cold-flow facility were completed during the quarter. A probe collar (See Figure II.H.1 in the 5th Quarterly Report) to make gas extractions from the flow was installed and tested. The probe collar enables sampling over the entire flow cross-section. The collar can be moved to various streamwise locations; thus, gas extractions can be taken at almost any axial location of interest in the flow. Modifications were also made to the smoke-generating device to increase the quantity of smoke yielded. The best results were obtained by heating a thin film of a commercial, smoke-producing fluid. It was found that if the fluid used to produce the smoke was allowed to accumulate on the heated surface, its decomposition was slowed and the amount of

smoke produced decreased. By increasing the heated area of the generator, and by tilting the smoke generator at an angle to avoid buildup of the fluid, adequate amounts of smoke were produced to visualize the flow.

An IR CO_2 analyzer was installed in the cold-flow facility, connected to the sample probe collar, and calibrated. CO_2 is being injected into the flow chamber through the crossflow jets and the IR analyzer will be used to determine the local composition of gas samples extracted from the flow. The relative concentration of CO_2 in the mixed gases is a direct measure of the extent of mixing in the duct at the local sample point.

Checkout testing was initiated during the quarter to identify possible problems with the apparatus, and to gain familiarity with the flow control and metering devices. Preliminary tests using smoke injection showed a strong recirculation zone at the inlet of the main flow chamber. This recirculation zone was also observed by previous researchers using the cold-flow facility (see Lindsay et al., 1986). It may be necessary to install a flow straightener in the main flow chamber if the recirculation zone proves to have a significantly distorting effect on the mixing of the crossflow jets.

Testing with CO_2 tracer gas injection was also initiated. Preliminary results showed a significant increase in the mixing rate when using three crossflow jets versus a single jet, while keeping the total jet flowrate constant. Extractions were made over cross-sections of the flow and analyzed for their CO_2 concentration. Figure II.H-1 shows the normalized concentrations obtained at a point near the tube wall. Note that the configuration with three injection jets approaches the well-mixed value much more rapidly than that from the configuration with a single injection jet, even though the total mass of the material injected was the same. With the three jets, the well-mixed concentration at that sample point was reached by about 5 duct diameters, whereas the injection with one jet required about 7.5 duct diameters to reach the well-mixed level.

Figure II.H-2 shows the normalized trace gas concentrations obtained at the centerline of the flow chamber. Extractions taken at the centerline seem to indicate that the single jet configuration mixes more rapidly; however, the additional velocity used for a single jet at the same total flowrate as three jets, forces the injected gases to penetrate farther into the main flow. This penetration raises the centerline concentration, while other areas of the flow are not as well mixed. Over the entire cross-section of the flow, the three-jet configuration has been observed to mix better than the single-jet configuration for all cases tested thus far. Complete maps of concentration (and consequently mixing pattern) will be obtained during the next reporting period.

Component 2 - Laboratory-Scale Reactor Modifications

This subtask component is aimed at modifying the laboratory-scale reactor to accommodate sorbent particle injection. Previous research has shown (see Categen et al., 1987; and Kamotani and Gerber, 1974) that the two most important criteria in the mixing of crossflow jets are the jet-to-main flow diameter and momentum flux ratios. The effect of both criteria will be investigated in these experiments. The lower limit of the sorbent/sulfur ratio will be determined by the amount of sorbent which can be entrained in a given amount of gas while maintaining an adequate sorbent/sulfur ratio, and the upper limit will be

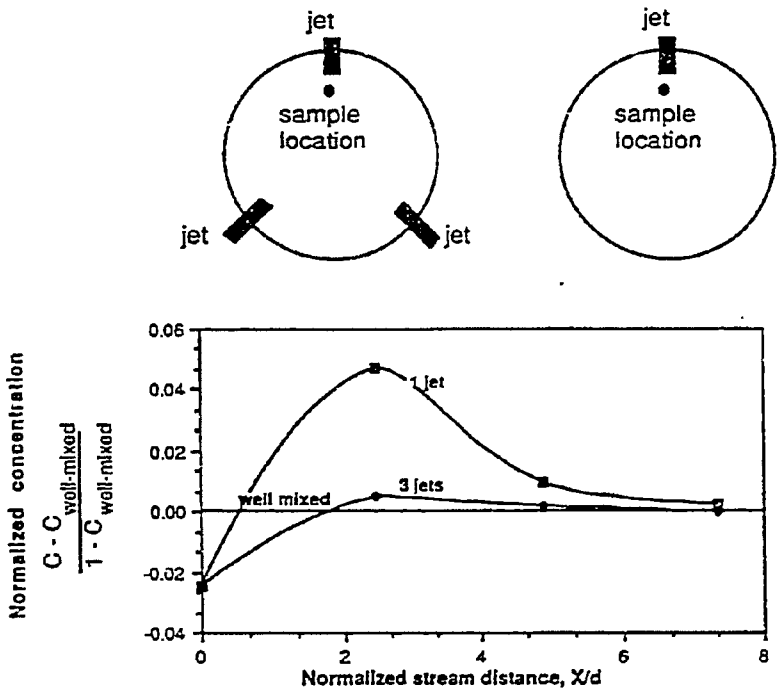

Figure II.H-1. Near-wall concentration of tracer gas.

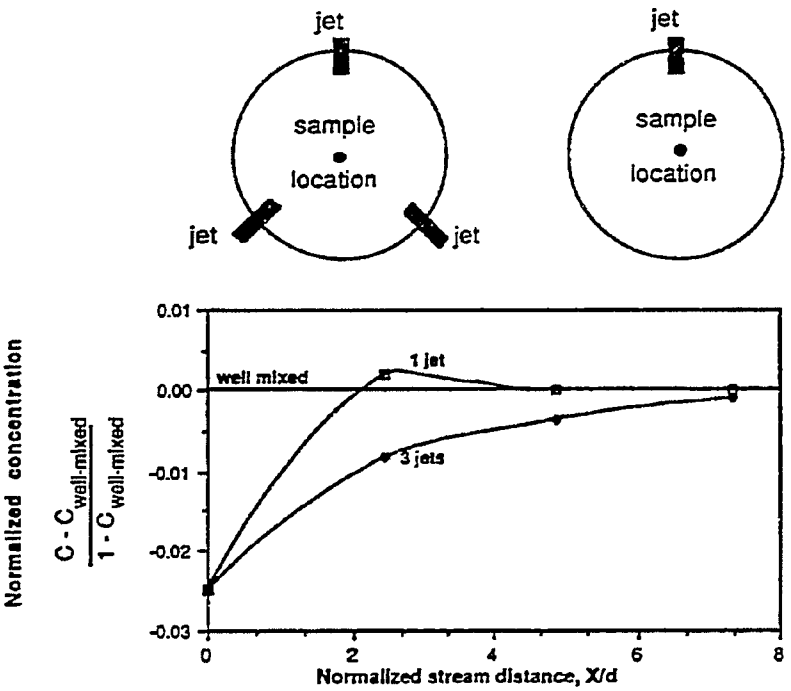

Figure II.H-2. Centerline concentration of tracer gas.

determined by the amount of gas and sorbent flow which would overly dilute the gasifier effluent. One of the modular reactor sections is being modified to allow the sorbent to be injected perpendicularly to the main gasifier flow through three injection ports uniformly positioned around the circumference of the reactor section. In addition, it has been necessary to design and construct a new pressurized feeder for sorbent injection, and to connect the feeder to an inert gas flow system that will be used to transport the sorbent to the crossflow injectors.

During the reporting period, the research team has worked on the maintenance and repair of the existing facilities while designing and manufacturing the necessary new facility components. The new components include: the pressurized sorbent feeder, the modified reactor section for the injection of the sorbent particles, and the flash tank.

The pressurized sorbent feeder (Figure II.H-2 in the 5th Quarterly Report) has been completed and is ready to install. Sorbent will be injected through three equally-spaced ports in a modified reactor section. Figure II.H-3 shows a schematic of the modified section. Tests conducted in the cold-flow facility have shown that three ports spaced 120 degrees apart will provide good mixing between the sorbent particles and the pollutant species.

A flash tank has also been designed and manufactured for the facility. A schematic of the completed flash tank is shown in Figure II.H.4. The flash tank will allow the noxious sulfur and nitrogen pollutant gases, that are dissolved in the exhaust gas quench water when tests are conducted at elevated pressures, to be separated from the quench water and be discharged to the exhaust gas flare on the roof of the laboratory building. This will eliminate a problem with the noxious exhaust gases being discharged to the sewer and being vented back into occupied work areas.

Work has also been conducted on to modify the gasifier so that temperature measurements of the gases inside the reactor can be measured. In the past, thermocouples have not been inserted into the reaction chamber due to the high temperatures and highly corrosive atmosphere, but were embedded into the insulating refractory wall. High-temperature thermocouples have been ordered, and by adjusting the thermocouple ports, temperature measurements within the reactor effluent will be attempted. It is not certain if these temperature measurements can be related to the local gas temperature, but an attempt to do so will be made. Also, a reactor section will be modified to incorporate two quartz sight windows spaced 180 degrees apart to allow the use of an FTIR analyzer (supplied by AFR) from which temperature profiles and gas species concentrations will be obtained. The use of the FTIR will be somewhat limited by the limited optical transmission of the quartz windows used in the reactor sight windows to the near-IR region (to ca. 2.7 microns). Nevertheless, important temperature and species concentration data for verification of the computer code will be obtained.

Several familiarization and checkout tests have also been conducted with the facility. The familiarity with the equipment and procedures gained in these tests will be invaluable during the test period. Some of the highlights include: on February 23, 1988 the gasifier was operated with Illinois No. 6 coal at atmospheric pressure; on March 17 the gasifier was operated with Utah coal at atmospheric pressure, and on April 7 the gasifier was operated with Utah

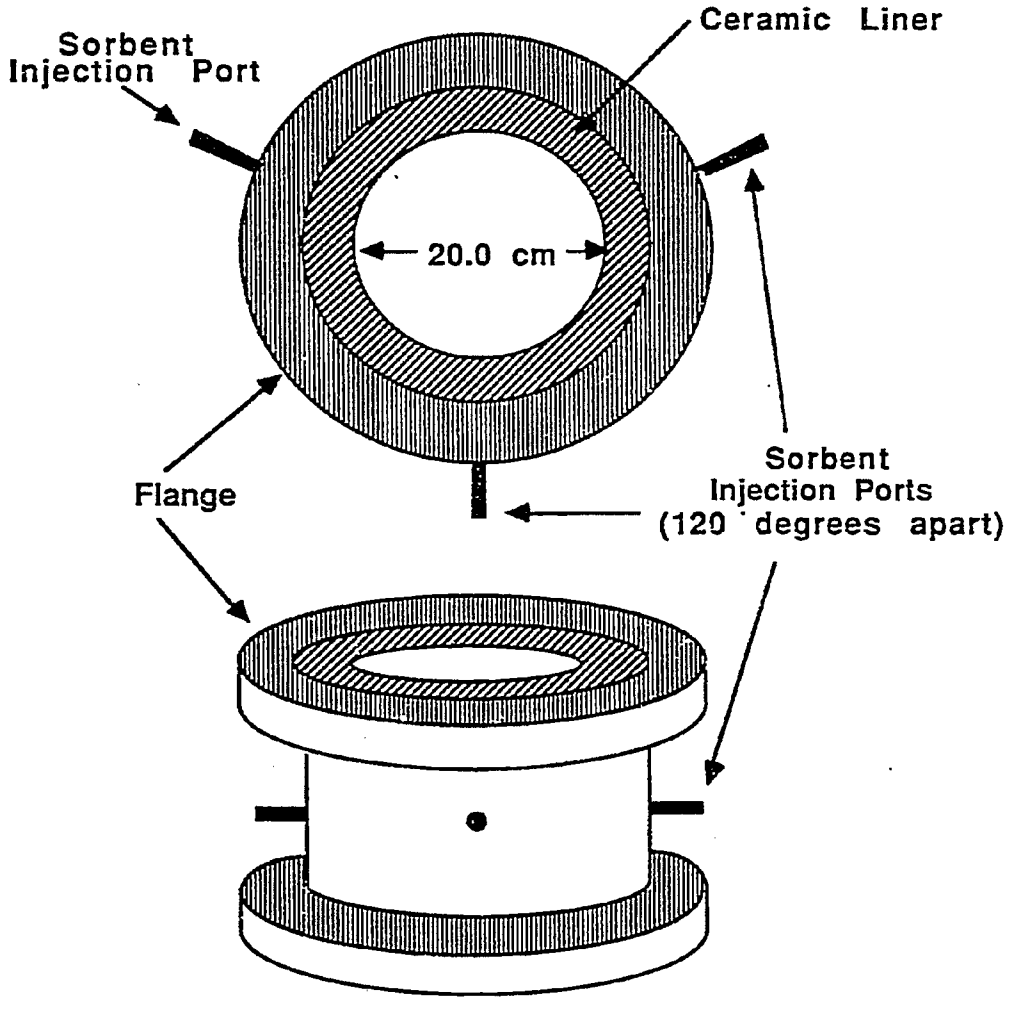

Figure II.H-3. Modified reactor section for the injection of sorbent particles from three ports.

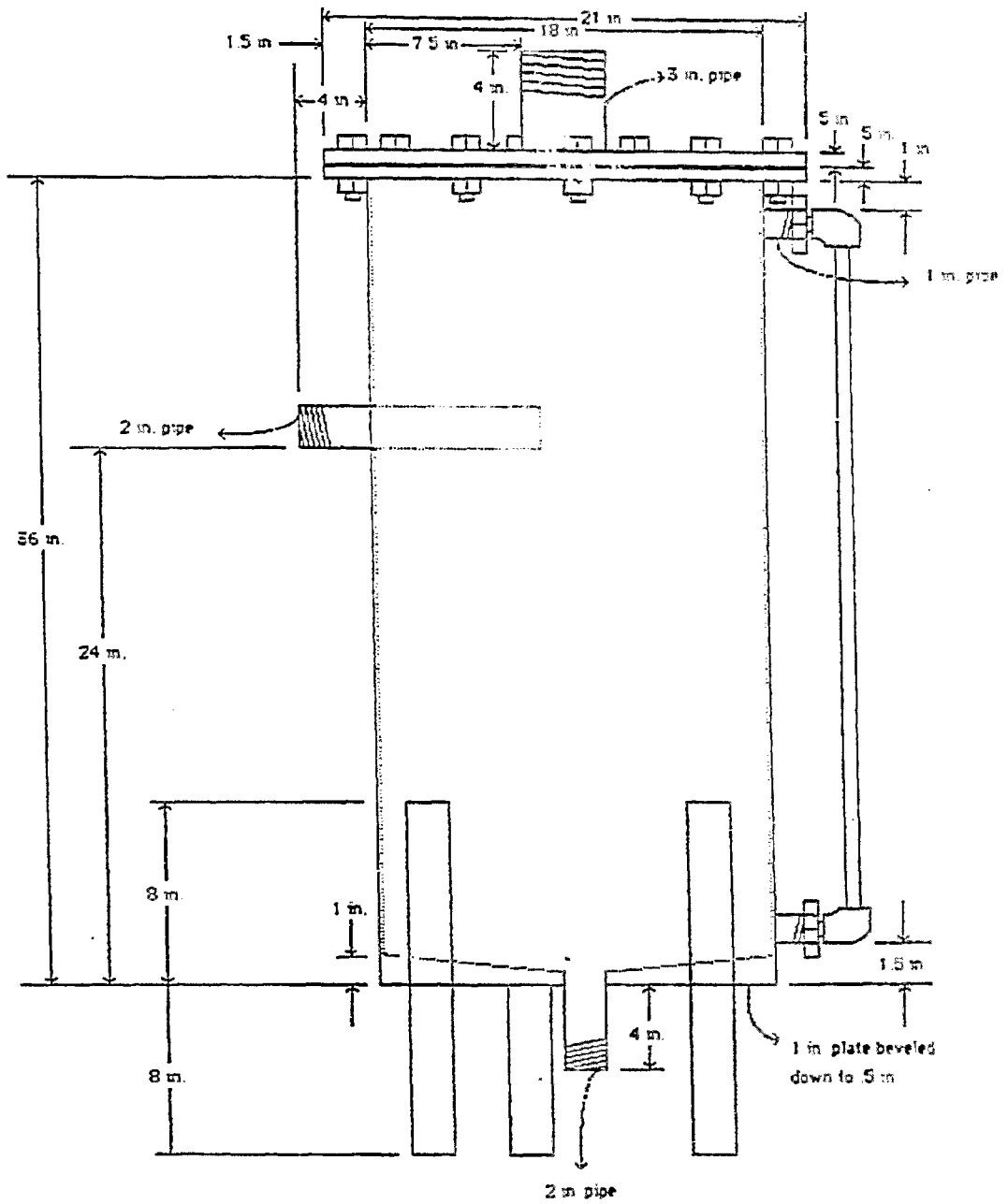

Figure III.H-4. Schematic drawing of the absorbed pollutant flash tank.

coal at 5 atmospheres of pressure. Repairs and maintenance of the facility have continued as these tests have been conducted.

During the recent contract review meetings between BYU and AFR, it was recommended that tests be conducted with a higher rank coal along with the two bituminous coals, Utah (low sulfur content) and Illinois No. 6 (high sulfur content), that are already on hand. Efforts have been made to obtain a source of Pocahontas No. #3 which will be added to the test matrix. A supply of sorbent (approximately 96% calcium carbonate) has been obtained and is now being prepared and analyzed in preparation for the test program.

Component 3 - Space-Resolved Sulfur and Nitrogen Pollutant Measurements

This subtask component is aimed at making detailed measurements of sulfur and nitrogen pollutants and char in the laboratory-scale reactor. Work on this subtask will follow the completion of Component 2.

Plans

Component 1 - Sorbent Mixing Fluid Mechanics

Testing using CO_2 tracer gas injection will continue. The test program will investigate the effect of the number of jets, jet-to-main flow size ratio, jet-to-main flow momentum ratio, and streamwise location of the jets on mixing. Testing will also be done at different Reynolds numbers in the simulated gasifier effluent to determine how the intensity of the turbulence affects the jet mixing. Additional testing using smoke injection will be conducted to obtain qualitative information about the flow and mixing patterns, and different methods of presenting the results observed using smoke will be investigated. Laser doppler anemometer (LDA) tests will determine mean and instantaneous flow velocities.

Component 2 - Laboratory-Scale Reactor Modifications

One additional checkout test is planned. This test will be made with the direct injection of a mixture of coal and sorbent particles into the gasifier. This test will determine if the introduction of the sorbent causes any unusual problems with the formation of slag in the reactor, and if the slag formed might cause any unforseen problems with the refractory insulation. Once this checkout test has been completed, the flash tank, pressurized sorbent feeder, and injector system will be installed. The reactor will be completely disassembled, and new refractory insulation will be installed. This is being done to prevent any possible sulfur contamination from earlier experimental tests with high sulfur coals from interfering with the sorbent capture tests.

Work will be continued, to prepare the coal and sorbent (dry, pulverize and analyze), to improve the ignition system, and to implement analysis techniques for sorbent particles. Routine testing is scheduled to begin in early May. A joint test with AFR will be made later in the summer. AFR will bring their FTIR instrument to BYU, where it will be used to make temperature and species measurements across the flame front in the gasifier. For this test, one of the reactor sections will be further modified to allow optical access from both sides of the reactor.

Component 3 - Space-Resolved Sulfur and Nitrogen Pollutant Measurements

Once the Component 3 experiments are completed, space-resolved sulfur and nitrogen pollutant measurements with or without sorbent injection will be made.